Rational Analysis and Design of Prestressed Concrete Beam Columns and Wall Panels

Noel D. Nathan
Professor of Civil Engineering
University of British Columbia
Vancouver, British Columbia
Canada

Precast concrete columns are often cast and shipped in lengths extending over two, three, or more stories. In consequence, they are frequently long and slender, at least until jointing is complete, so that handling stresses may give rise to problems.

Similarly, precast loadbearing wall panels for light industrial or warehouse structures are generally required to be very tall, again leading to high slenderness ratios. The roof loads, distributed along the wall, are usually quite light, so that stress conditions are often dominated by the bending moments arising from wind loads and load eccentricity.

For the above reasons, precast columns and loadbearing walls are frequently prestressed.

Codes of practice usually provide empirical formulas for the effects of slenderness, but limit the range of slenderness for which they may be used. For example, ACI 318-83[1] requires that if the slenderness ratio L/r exceeds 100, design shall be based on analysis which "shall take into account influence of axial loads and variable moment of inertia on member stiffness and fixed-end moments, effect of deflections on moments and forces, and the effects of duration of loads." No direct guidance, however, is given on how to make such an analysis.

Precast prestressed concrete columns and wall panels frequently fall within the range of slenderness that excludes use of the empirical formulas. Furthermore, it has been found that the empirical formulas are not as precise for the

very low percentages of steel that are generally present in precast members, even when the slenderness ratios are small.

This paper will address these problems by reviewing the analysis for secondary effects in columns and walls. Methods involving varying degrees of approximation will be briefly discussed. The effect of prestressing will be reviewed, and it will be suggested that rational analysis of components should generally be the preferred approach for precast prestressed elements.

The theory of such a rational analysis will be developed. The construction of a computer program typical of those used by researchers for this purpose will be briefly described. A listing and documentation of the program can be obtained at cost of reproduction from the Prestressed Concrete Institute.

The computer program may be used to determine the design moments for a given set of loads and end conditions, or to develop design curves of acceptable loading for given member cross sections and will predict material or instability failure. The cross section may have any polygonal shape and may have any number of mild steel bars and/or prestressing tendons. The concrete and steel components may have any stress-strain laws, specified in functional form or in the form of points on an experimentally determined curve.

Any form of lateral loading can be handled, specified by the primary bending moment arising therefrom. The axial load may be applied with different eccentricities at the two ends. Initial curvature may be included.

Note that the boundary conditions must be known or an effective length must be estimated. A load-deflection analysis is used to account for lateral displacement of the joints if such displacement is permitted.

It is recommended that precast concrete manufacturers use computer programs such as this to develop design curves for standardized products such as columns, double tees, piles, and other customized units. The author's program has been written in very elementary FORTRAN and therefore should be easily adaptable to specific needs.

Synposis

Secondary effects of axial loads on frame members are discussed. Methods of analysis for these forces are reviewed. Characteristics of prestressed concrete members which affect the method of analysis are described, and it is noted that "rational analysis" is often required. Construction of a computer program to perform such an analysis of component members is discussed, and a program is described in detail in an appendix. Several examples are included.

SECONDARY EFFECTS IN FRAMES

This section contains a brief discussion of the problems associated with axial loads in frame elements and of the methods of dealing with them.

The presence of axial compression in a frame member has two effects:

1. The stiffness of the member is reduced.
2. Secondary bending moments, not accounted for in the primary analysis, are generated when the line of action of the axial force is no longer coincident with the centerline of the member.

It is possible to make analyses which take all these factors into account, but difficulties are involved,[2,3] particularly in the design stage of reinforced or prestressed concrete frames. However, the first effect, namely, the reduction in

stiffness, is negligible if the axial load is a reasonably small proportion of the Euler load for the member.[3,4]

This condition is generally satisfied in practical building frames, so that the effect of stiffness loss on the distribution of internal forces may effectively be ignored. A method of accounting for loss of stiffness, given in Refs. 5 and 6, is referred to below.

The secondary bending moments arise from changes in the geometry of the structure which are not taken into account in the primary analysis. These effects may again be separated into two parts:

1. Relative motion of the joints with respect to one another, in the transverse direction to the axial loads. Erection tolerances may contribute to this effect.
2. Departure of the member centerline from the straight line between the joints, due to bending of the member along its length. Thermal bowing, manufacturing tolerances, and camber may be significant in this respect.

The response of a structure to loads, accounting for these effects, may be evaluated by a variety of procedures:

Method 1

An equivalent pin-ended member is assumed for each column. The "effective length" of this equivalent member depends upon the end conditions.[7] When sidesway is not prevented, the first of the effects noted in the previous paragraph is accounted for if the deflections are measured from the thrust line, and the column is given an imaginary extension, until it recrosses the thrust line at an imaginary point of inflection.

The response of this equivalent pin-ended member is then obtained by modifying the primary bending moment causing sway by a magnification factor. The moments not associated with sway are also magnified to account for the second effect, using the braced effective length.

Method 2

An approximate analysis is made to determine the horizontal displacements of the joints, and the so-called P-Δ (load-deflection) moments arising therefrom are directly calculated. The magnification factor is then used to account for the additional secondary moments due to deflection of the column centerline, using the effective length for a braced column.

Method 3

The procedures of Methods 1 or 2 are used, but the response of the equivalent column is determined by some rational procedure instead of by means of the semi-empirical magnification factor.

Method 4

The entire analysis accounting for all the nonlinear secondary effects is carried out by a rational procedure, as discussed in Refs. 2 and 8. As mentioned above, this process is far too complex for practical use in the design stage of concrete buildings.

COMMENTS ON ANALYTICAL PROCEDURES

In this section, further comments are made on the individual steps involved in the above procedures, namely, the determination of effective length, the calculation of P-Δ moments, and the use of magnification factors.

Effective Length

The bifurcation buckling load for an individual column with pure axial load is determined by the Euler load for a hinged column of effective length kL,

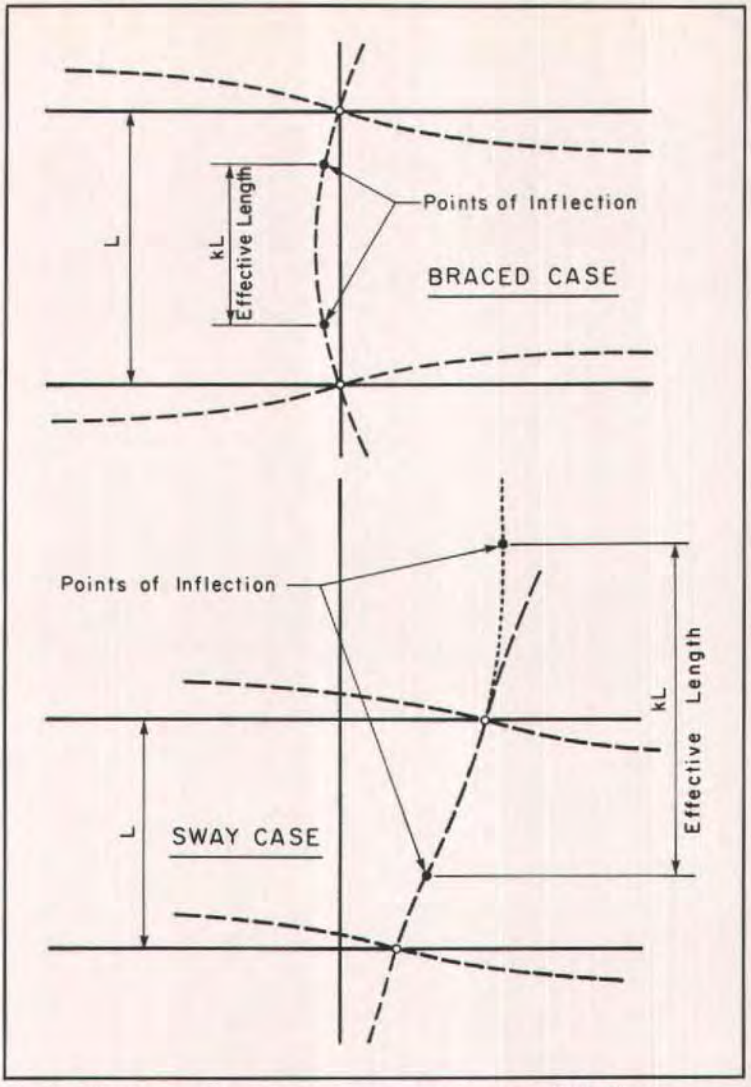

Fig. 1. Effective lengths of columns in a frame (after Ref. 9).

the distance between the points of inflection at the instant of buckling. In framed members (see Fig. 1) the effective length depends upon the relative stiffnesses of the columns and the restraining beams.

When moments or lateral loads are present, as is usually the case, instead of bifurcation buckling, magnified moments (i.e., added secondary moments) occur, leading eventually to material failure or to instability. The magnification, however, also depends upon the effective length and therefore on the restraint conditions at the ends of the column.

The determination of effective length is discussed in Refs. 3, 7, and 9. In practice, the Jackson-Moreland alignment charts[9,10] are generally used for this pur-

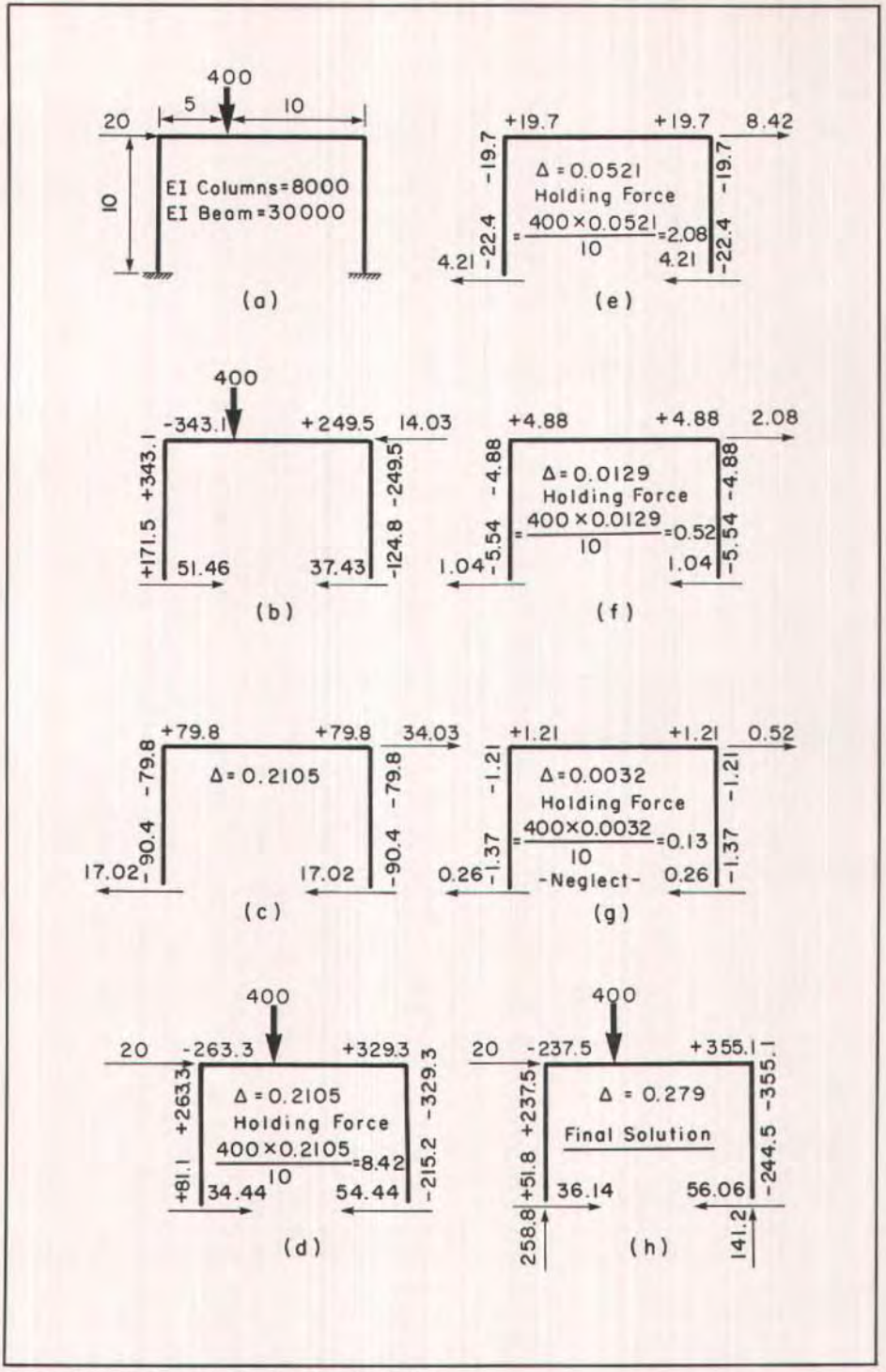

Fig. 2. Iterative load-deflection (P-Δ) analysis.

pose; k is often taken as unity when sway is not permitted.

The derivation of these charts is discussed by Galambos,[3] Kavanagh,[7] and Chu and Chow.[11] MacGregor and Hage,[12] however, assert that the charts are "based on highly idealized and quite impractical cases," and they show that they lead to unrealistic results — often highly conservative but occasionally unconservative.

The difficulties in using the effective length approach are associated with the evaluation of the restraining effects of the beams on the column, particularly in unsymmetrical structures, when sidesway takes place. It is for this reason that the P-Δ method[4,12] is advocated for the separate evaluation of the moments arising from sidesway.

Evaluation of P-Δ Moments

The application of various procedures for computing the effects of sidesway are excellently set forth in Refs. 5 and 12, and will be briefly discussed here.

An iterative procedure[4,5,12] will be illustrated by means of the simple portal frame shown in Fig. 2a. In Fig. 2b a first order analysis is made of the gravity loads. Sidesway is prevented by means of a holding force found to be 14.03. Fig. 2c shows the removal of that holding force together with the application of the lateral load of Fig. 2a.

The sum of Solutions 2b and 2c, shown in Fig. 2d, would complete the usual first order analysis. But now, the deflection ($\Delta = 0.2105$) is computed and it is deduced that the columns are acted upon by a moment $\Sigma P\Delta$ (i.e., 400 x 0.2105) which is not, as yet, balanced. Therefore, in order to maintain equilibrium, there must be a remaining holding force of:

$$\Sigma P\Delta/h = 400 \times 0.2105/10 = 8.42$$

The effect of removing this force is shown in Fig. 2e; however, there is then a further deflection of 0.0521 and therefore, by the same reasoning, a holding force of 400 x 0.0521/10 = 2.08. The effect of removing this force is shown in Fig. 2f, and it is seen that there is a further deflection of 0.0129 and a holding force of 0.52.

This leads to Fig. 2g, with deflection 0.0032 and holding force 0.13. This is considered negligible, and the solution is assumed to be the sum of Figs. 2d, e, f, and g. If the process does not rapidly converge, it indicates that the structure is probably too flexible with respect to sway.

Note that the solutions for Figs. 2e, f, and g are simply prorated from that of Fig. 2c. The whole procedure is usually an elastic analysis performed with respect to the factored loads; however, since it is an elastic analysis, it can often be obtained by factoring up the components of a service load analysis (similar to Figs. 2b and 2c) performed to check service load drifts. Note that if there are changes in the stiffnesses due to cracking as the factored loads are approached, this should be accounted for.[12]

The process illustrated in Fig. 2 is easily extended to the general case of multiple stories and multiple bays. It has accounted for the secondary moments arising from horizontal motion of joints, but moments arising from displacement of the member centerline between joints have yet to be accounted for by means of the magnification factor (based on the braced effective length), or by further rational analysis. Note that, even when sidesway is restrained, this process leads to the values of the forces in the wall or bracing providing the restraint.

If the increments of deflection in the preceding method are written out in symbolic form, it will be found that they form a geometric series whose sum is given by:[12]

$$\Delta_2 = \frac{H/K}{1 - \frac{\Sigma P}{Kh}} = \frac{\Delta_1}{1 - \frac{\Sigma P \Delta_1}{Hh}} \qquad (1)$$

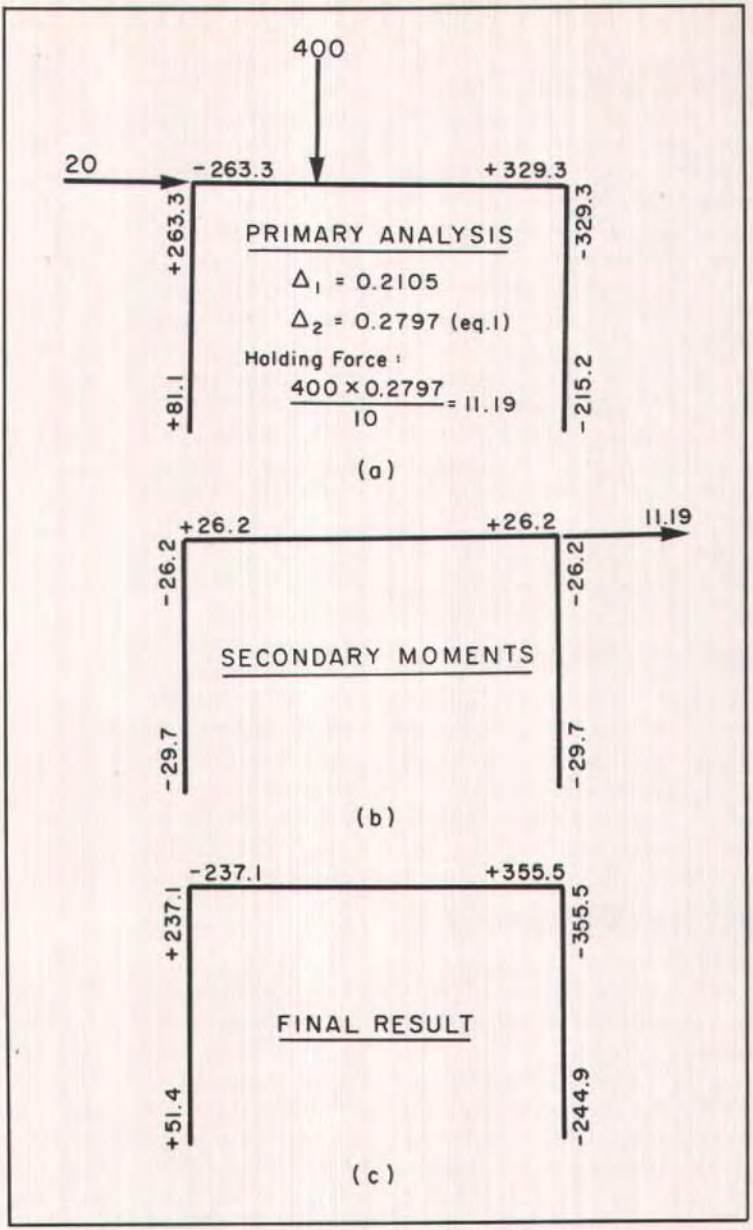

Fig. 3. Secondary analysis using series summation for deflection Δ.

or

$$\Delta_2 = \frac{0.2105}{1 - \frac{(400)(0.2105)}{(34.03)(10)}} = 0.2797$$

where

Δ_1 = primary deflection (Fig. 2c)
Δ_2 = final total deflection
H = sway force
K = lateral stiffness of frame

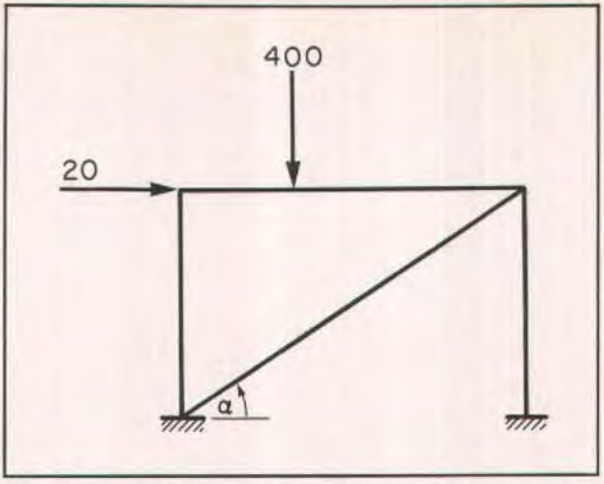

Fig. 4. Imaginary bracing providing secondary forces.[13]

Note that if the numerator is equal to or less than zero, the series does not converge and the structure is unstable. In this way, the total deflection is obtained without iteration, and the total holding force from Figs. 2e, f, g follows immediately. One more elastic analysis under this force gives the final result (see Fig. 3).

This procedure is strictly valid only for single story frames, but it can be used for multistory structures in which there are points of inflection in the columns (relatively stiff beams) and in which the magnification is of the order of 1.5 or less.[5]

Finally, an ingenious method suitable for computer analysis of large frames, presented by Nixon, Beaulieu, and Adams,[13] will be described.

Suppose, as before, that the final lateral deflection of the structure in a given story is Δ_2, giving rise to total column moments $\Sigma P\Delta_2$. As shown above, an additional horizontal force $\Sigma P\Delta_2/h$ in the direction of Δ_2 would cause these moments.

Now suppose that an imaginary bracing member is added as shown in Fig. 4 with stiffness such as to cause the force $-\Sigma P\Delta_2/h$ when there is relative lateral displacement Δ_2. (Negative because the member must exert a force in the same direction as its deformation.) The stiffness of the bracing member with respect to extension along its axis is AE/L, so that the stiffness with respect to horizontal displacement is $(AE/L)\cos^2\alpha$. Thus:

$$\frac{AE}{L}\cos^2\alpha\,\Delta_2 = -\frac{\Sigma P\Delta_2}{h} \qquad (2)$$

or

$$A = -\frac{\Sigma PL}{Eh}\frac{1}{\cos^2\alpha}$$

where L is the length of the bracing member.

That is, if imaginary bracing members are inserted in each story, with negative areas as given by this equation, they will lead to correct moments in the columns and beams. The shears and axial forces will be somewhat in error due to the forces in the bracing, but these effects will be quite small[13] (the negative areas required are, in fact, very small), and they can be minimized by making the bracing angle α as flat as possible. One bracing member per story can stretch across all the bays of the frame. This

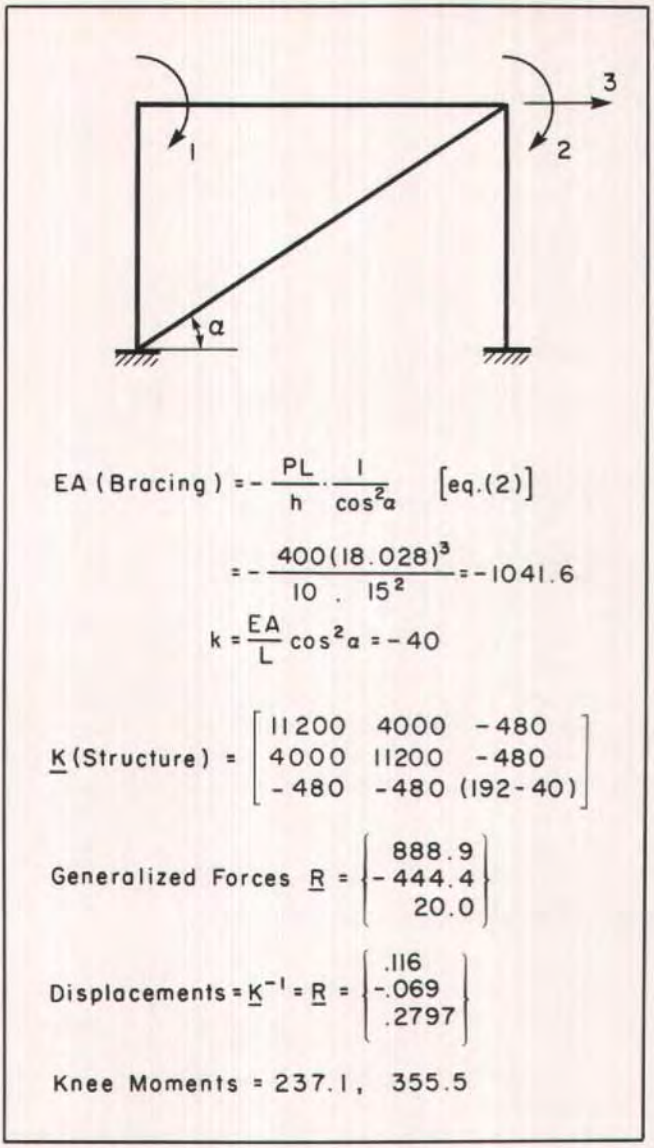

$$EA\,(Bracing) = -\frac{PL}{h}\cdot\frac{1}{\cos^2\alpha} \quad [eq.(2)]$$

$$= -\frac{400(18.028)^3}{10\ .\ 15^2} = -1041.6$$

$$k = \frac{EA}{L}\cos^2\alpha = -40$$

$$\underline{K}\,(Structure) = \begin{bmatrix} 11200 & 4000 & -480 \\ 4000 & 11200 & -480 \\ -480 & -480 & (192-40) \end{bmatrix}$$

$$\text{Generalized Forces } \underline{R} = \begin{Bmatrix} 888.9 \\ -444.4 \\ 20.0 \end{Bmatrix}$$

$$\text{Displacements} = \underline{K}^{-1} = \underline{R} = \begin{Bmatrix} .116 \\ -.069 \\ .2797 \end{Bmatrix}$$

$$\text{Knee Moments} = 237.1,\ 355.5$$

Fig. 5. Second order analysis using bracing with negative area.

procedure, shown in Fig. 5, can be used in a standard frame analysis program without modification.

The loss of stiffness in the column members can be accounted for in each of the foregoing P-Δ analyses by including a "flexibility factor" in the term ΣP. This factor, developed in Ref. 5, is given by:

$$\gamma = 1 + 0.22\left\{\frac{4(\psi_A-\psi_B)^2 + (\psi_A+3)(\psi_B+3)}{[(\psi_A+2)(\psi_B+2) - 1]^2}\right\} \qquad (3)$$

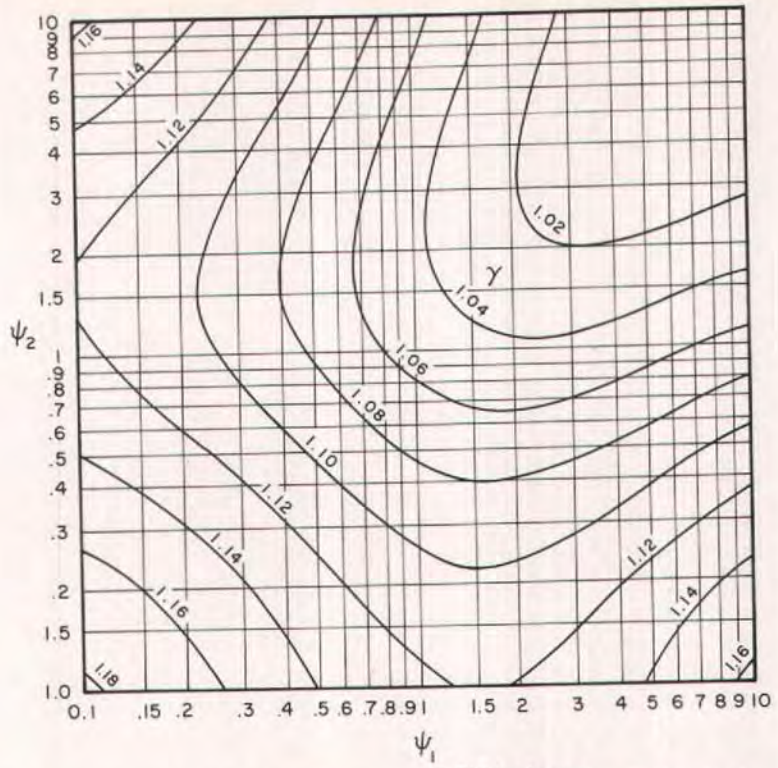

Fig. 6. Flexibility factor γ of Eq. (3). $\psi_i = \dfrac{(\Sigma\, EI/L)\text{columns}}{(\Sigma\, EI/L)\text{beams}}$ at End i of column.

where

$$\psi = \frac{\left(\Sigma \frac{EI}{L}\right)_{col.}}{\left(\Sigma \frac{EI}{L}\right)_{beam}} \text{ at End A or B of column}$$

The ψ factor varies between 1 and about 1.2, and values are given in Fig. 6. Inclusion of this factor gives a good estimate of the lateral deflections, although the redistribution of the moments is not properly accounted for.

Magnification Factor

It is shown by Galambos (pp. 246-7 of Ref. 3) that the moments in a column bent in single curvature are magnified, due to displacements with respect to the thrust line, by the factor:

$$\delta = \frac{1}{1 - P/P_E} \qquad (4)$$

Eq. (4) is essentially the same formula used in the ACI Building Code.[1] When the effective length for the sway case as illustrated in Fig. 1 is used, this magnification factor includes the P-Δ effects discussed above, since the displacement from the thrust line includes the Δ deflection. However, it will be observed that the additional moments of Figs. 2d, e, f, and g all arise from the conditions of Fig. 2c, and are quite independent of Fig. 2b (except insofar as the holding force of 14.03 is concerned).

Thus, the magnification factor associated with the sway-permitted effective length applies only to the moments arising from sway forces (Fig. 2c). This is made clear in Ref. 1, where the mag-

nified factor moment in a column is:

$$M_c = \delta_b M_{2b} + \delta_s M_{2s} \qquad (5)$$

in which

M_{2b} = value of larger factored end moment on compression members due to loads which result in no appreciable sidesway, calculated by conventional elastic analysis

M_{2s} = value of larger factored end moment on compression member due to loads which result in appreciable sidesway calculated by conventional elastic frame analysis

Note that δ_b and δ_s, discussed below, are based on the effective length for the braced and unbraced cases, respectively.

It is recognized that the two components of M_c in Eq. (5) do not necessarily occur at the same point in the column, and are therefore not directly additive. Nevertheless, the true maximum cannot be greater than their sum, so, for the sake of simplicity, this conservative form is accepted.

The same problem arises more acutely when braced columns are subject to double curvature. In that case, the maximum secondary moment certainly occurs at a point remote from the maximum primary moment at the end of the column. The magnification factor should then include a factor $C_m \leq 1$. The theoretical value of C_m for elastic columns is given in Ref. 3, p. 246, together with various approximations, including that used in Ref. 1:

$$C_m = 0.6 + 0.4\,\frac{M_1}{M_2} \geq 0.4 \qquad (6)$$

Finally, noting that, due to diaphragm action of the floors, the displacements of all columns are essentially equal at floor levels, so that the sway magnification factors are the same for all columns of one story:

$$\delta_b = \frac{C_m}{1 - P_u/\phi P_c} \geq 1 \qquad (7a)$$

$$\delta_s = \frac{1}{1 - \dfrac{\Sigma P_u/\phi}{\Sigma P_c}} \geq 1 \qquad (7b)$$

where the summations are over all the columns of the story.

$$P_c = \frac{\pi^2 EI}{(kL)^2} \qquad (8)$$

In calculating P_c, the value of k is obtained from the Jackson and Moreland charts for the braced and unbraced cases. Approximate formulas are given[1] for the rigidity EI which represent behavior as the ultimate load is approached.

An interesting result from Ref. 14 shows that the critical load for any floor of a frame is:

$$\Sigma P_c = \frac{Hh}{\gamma \Delta} \qquad (9)$$

where

Δ is the deflection from a first-order analysis.

γ depends upon the deflected shape of the columns. Its numerical value lies between 1 and 1.22. [See Eq. (3) and Fig. 6.]

If one takes $\gamma = 1$, then:

$$\delta_s = \frac{1}{1 - \dfrac{\phi \Sigma P_u \Delta}{Hh}} \qquad (10)$$

The deflection Δ should be obtained from a primary analysis of the sway effects, presumably using the rigidity EI specified for use in P_c.

MacGregor and Hage[12] present step-by-step procedures for the use of these methods in the design process. For example, one may begin with δ_s from Eq. (10) based on the permissible drift index Δ/h and end with column size selection to ensure that the permissible index is not exceeded.

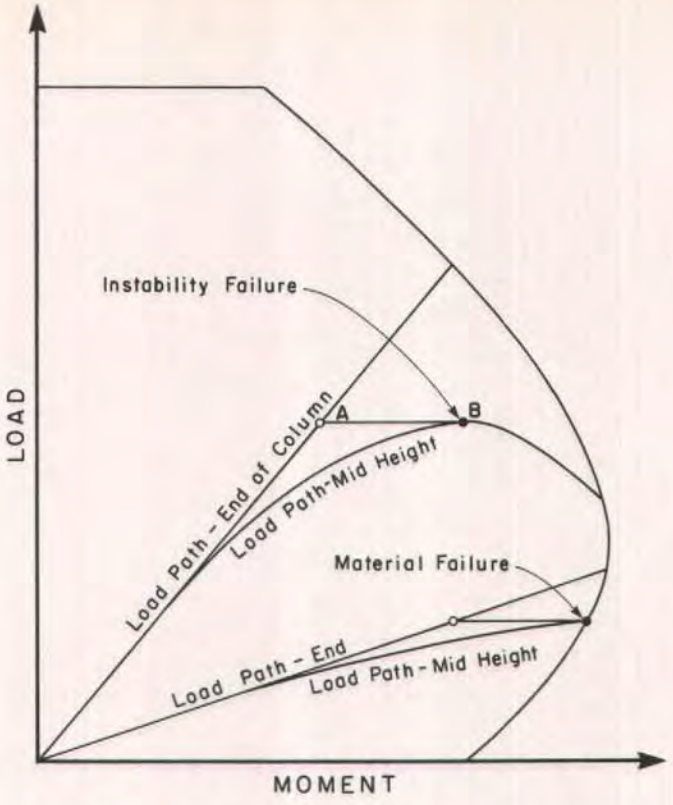

Fig. 7. Instability failure and material failure.

APPLICATION TO PRESTRESSED CONCRETE

It has been shown[15] that, since they generally have a very low steel ratio, prestressed concrete members have different moment-curvature relationships from normal reinforced concrete members. As a result of this, they are governed by instability rather than by material failure for almost the entire range of slenderness values. Furthermore, they are often used at higher slenderness ratios, which compounds the problem.

The P-Δ analyses discussed previously are not directly applicable when instability governs. It is assumed in those analyses, in removing the holding forces (Figs. 2d, e, f, g), that a linear analysis at the tangent stiffness of the structure is possible. The total moment, including the P-Δ contribution and the braced column magnification factor, is compared with short column capacity.

If the columns become unstable before reaching material failure the analysis becomes more complicated (see Fig. 7). MacGregor and Hage[12] caution against this possibility, giving criteria by which its likelihood may be assessed; but they note that it is seldom encountered in reinforced concrete building frames. When it is, the analysis of Fig. 2 must be modified to account for the loss of stiffness along the lines indicated in Refs. 16 and 17, or the γ factor of Eq.(3) can be included in the magnification factors to correct the deflections.

The susceptibility to unstable behav-

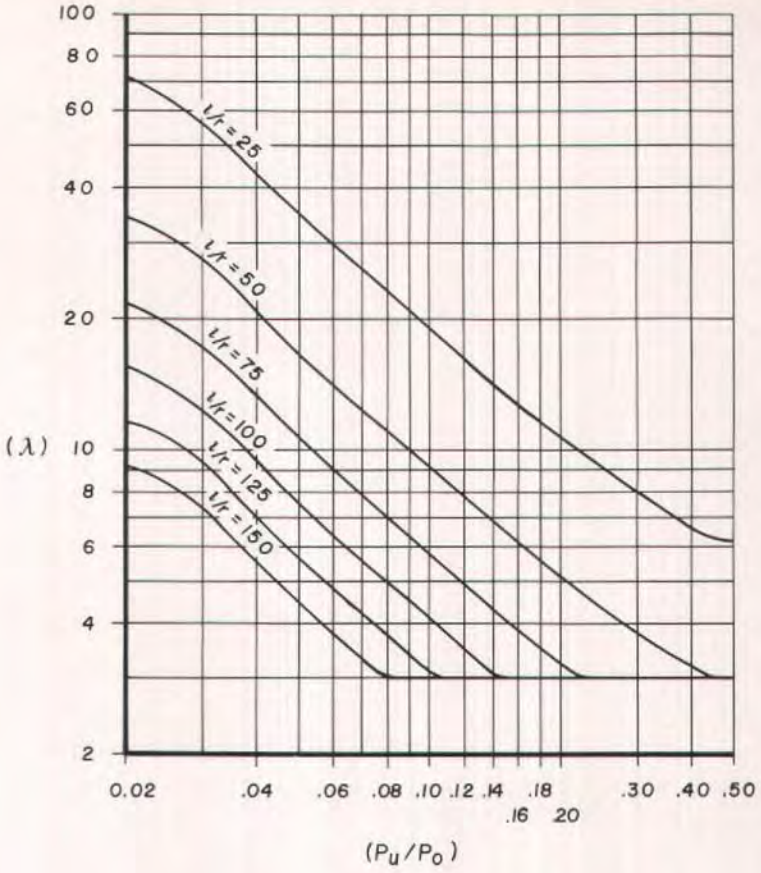

Fig. 8. Design aid for λ adjusted for use with ACI Code strength reduction factor and load duration factor $0 \leq \beta_d \leq 0.5$. Sections with no compression flange.

ior in members with very low steel ratios also leads to problems in evaluating the moment magnification due to deflection of the member centerline between joints.

Attempts have been made to extend the range of applicability of the ACI magnification procedure[1] to members with low steel ratios and high slenderness ratios. Using the theoretically accurate loads generated by the computer program detailed below, an effective rigidity EI was back-calculated for use in the computation of P_c:

$$EI = E_c I_c / \lambda(1 + \beta_d) \qquad (11)$$

with

$\lambda = \eta\theta \geq 3.2$

β_d = ratio of maximum factored dead load moment to maximum factored total load moment (always positive)

$$\eta = 2.5 + \frac{1.6}{P_n/P_o} \text{ where } 6 \leq \eta \leq 70$$

$$\theta = \begin{cases} \dfrac{35}{L/r} - 0.09 & \text{for sections with compression flange} \\ \dfrac{27}{L/r} - 0.05 & \text{for sections with no compression flange} \end{cases}$$

Design charts for λ are shown in Figs. 8 and 9.

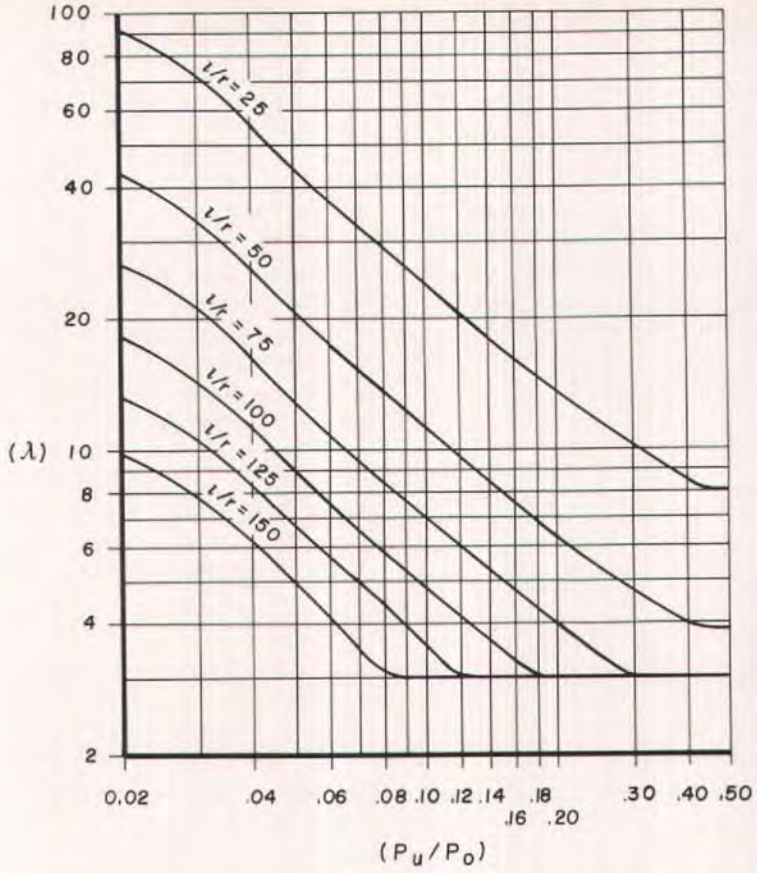

Fig. 9. Design aid for λ adjusted for use with ACI Code strength reduction factor and load duration factor $0 \leq \beta_d \leq 0.5$. Sections with compression flange.

The artificial nature of these factors must be emphasized. In the first place, sections with highly nonlinear moment-curvature relationships are being represented by a formula derived from linear material behavior (see Ref. 15, Fig. 14). Further difficulties arise from the application of the strength reduction factor ϕ, and with the long-term load factor β_d.

Together, these two factors account for variations in Young's modulus (due to creep and accidental variations), and for accidental variations in the moment of inertia and strength of the cross section. With regard to slenderness effects, all the section properties are reflected in the moment-curvature relationship.

It is presumed that the effects of ϕ and β_d should be to modify the moment/curvature relationship as shown in Fig. 10. For reinforced concrete columns with steel ratios of at least 1 percent and axial loads not too far below the "balanced" value, the moment-curvature relationship tends to be of Type A in Fig. 10. The influence of the ϕ and β_d factors is then accurately represented by applying them as in Eqs. (7) and (11). For the members with low steel ratios and axial loads presently under discussion, the moment-curvature relationships are of

Type B in Fig. 10, and the influence of the ϕ and β_d factors is not properly accounted for when they are inserted as shown in Eqs. (7) and (11).

In order to retain the traditional form of these equations, therefore, it is necessary to modify the quantities η and θ still further to the forms given in Eq. (11) above. These are to be applied with the ACI Code value of the ϕ factor and with β_d from 0 to 0.5. To predict the actual capacity of a cross section with $\phi = 1$ and $\beta_d = 0$, the expression given in Ref. 15, p. 68, should be used.

Since it is intended to cover a wide range of cross sections and design parameters, Eq. (11) is often very conservative. However, prestressed elements, particularly when precast, usually involve a good deal of repetition, since that is often the economic justification for their use.

This fact, coupled with the growing availability and declining cost of computers, suggests that a rational analysis would be appropriate for the development of the magnified moments. Manufacturers of standardized items could easily supply load capacity charts that include slenderness effects, and specialized items can be quite economically analyzed if reliable programs are available.

An advantage of precast prestressed

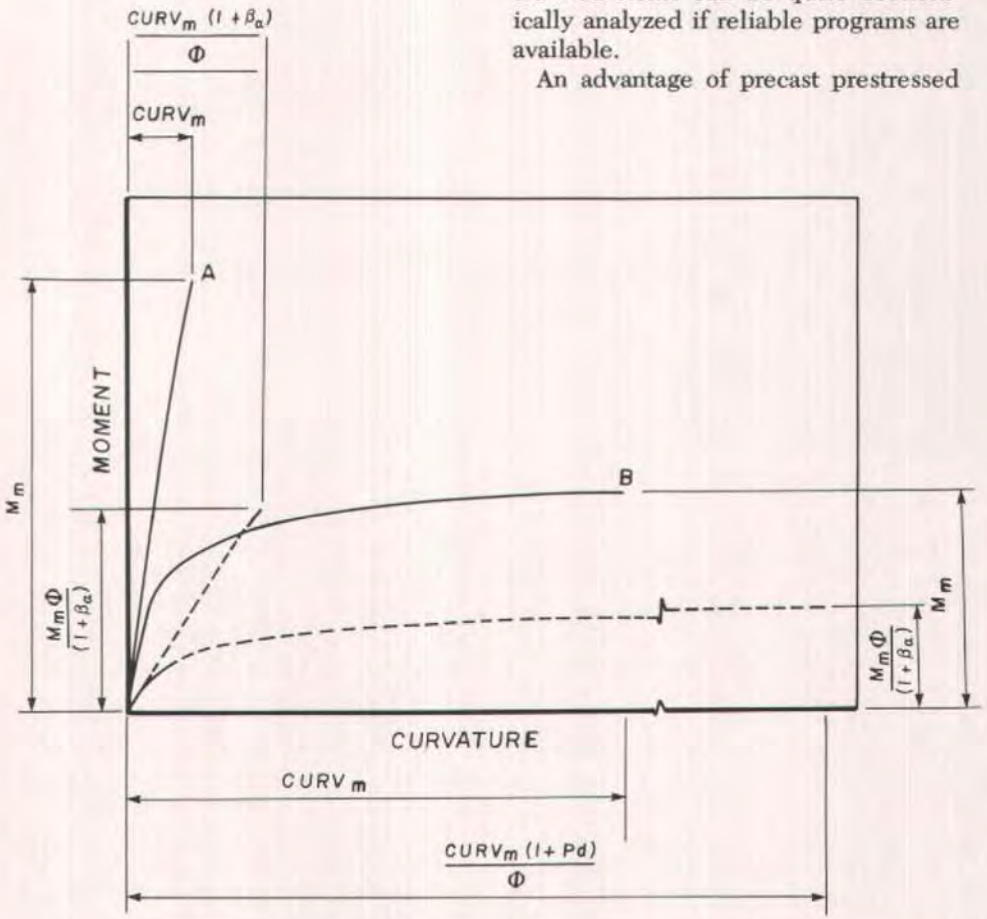

Fig. 10. Application of strength reduction factor and load duration factor to moment-curvature relationships. Heavily reinforced sections (A) and lightly reinforced sections (B).

piles and building members is that they are often statically determinate, or have reasonably well-defined boundary conditions, at least during the application of the dead loads (when they are often most vulnerable). Thus, one can frequently apply the effective length method, whether or not sidesway is prevented.

In summary, the application of the P-Δ methods to prestressed concrete should be made with caution, in that stiffness reduction may have to be considered. In applying magnification factors, whether to account for both P-Δ moments and deformation of the member between joints, or only for the latter, the usual procedures have been found to be less reliable than they are for normal reinforced concrete members. However, the repetition associated with precast members and their simpler boundary conditions favor the application of effective length methods with computer analysis of magnification effects.

The remainder of this paper will be concerned with the rational analysis of secondary moments in prestressed members with known effective lengths or boundary conditions.

OUTLINE OF RATIONAL ANALYSIS PROCEDURE

In this section, the essential steps in the rational analysis of a beam column with known boundary conditions (Ref. 3, p. 254) are defined.

The external moment at any point in a beam column (Fig. 11) is given by the primary moment (M_o) arising from the end moments and lateral loads, plus the secondary moment given by the axial load times the centerline displacement:

$$M_{ext}(x) = M_o(x) + Pv$$

The internal moment of resistance depends upon the axial load and the curvature, namely, the P-M-ϕ relationship. This is a complex function of the material properties, including the in-

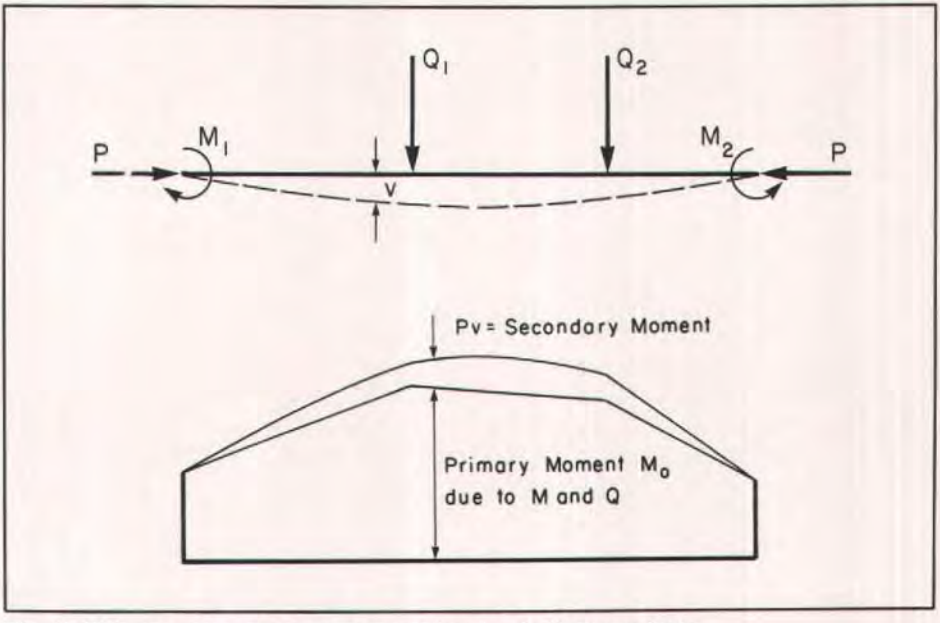

Fig. 11. Primary and secondary moments in a loaded beam column.

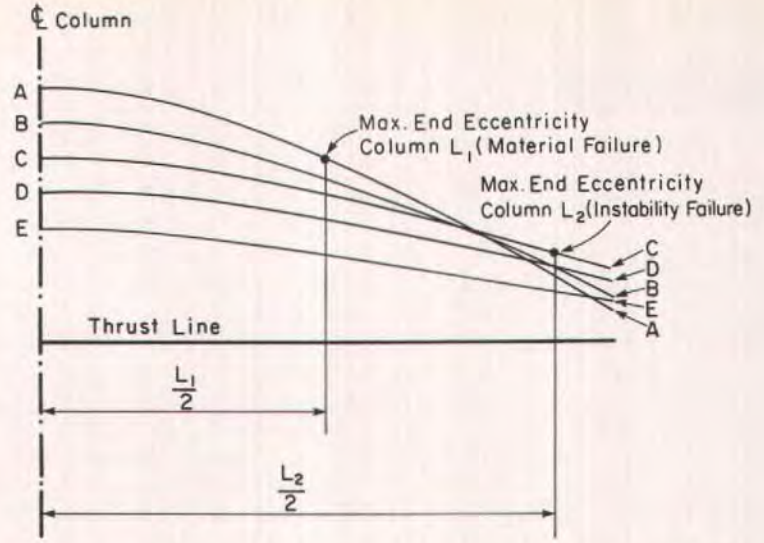

Fig. 12. Column deflection curves — Equal end eccentricities, single curvature.

elastic range up to failure, and the member cross section. The curvature, in turn, is a function of the centerline displacement and its derivatives, and, for small displacements, may be approximated by v''. Thus:

$$M_{int}(x) = f$$
$$= f(P, v'', \text{material, section}) \text{ for small displacements } v$$

For equilibrium, therefore:

$$M_{ext}(x) = M_{int}(x)$$

or

$$M_o(x) + Pv = f(P, v'', \text{material, section}) \qquad (12)$$

The solution of this differential equation is usually required in one of the following forms:

- The maximum moment in the member, given the applied lateral and axial loads.
- The maximum axial load the member can sustain, given the applied lateral loads.
- The maximum eccentrically applied axial load the member can sustain.

In any case, the first step is the evaluation of the P-M-ϕ relationship for the given cross section and the appropriate material properties (having regard for duration of loading, for example), giving the function $f(P, v'', \text{material, section})$.

It is recommended here that the solution of the differential equation then proceed by means of the numerical procedure set forth in Ref. 3, p. 279, or Ref. 18, p. 171. Starting with the prescribed boundary conditions at one end (usually displacement and moment), the remaining condition (usually slope) is assumed, and the solution curve is evaluated at successive nodes along the member by assuming a circular curvature within each short segment. The starting slope is adjusted and the procedure repeated until the prescribed boundary conditions at the far end are satisfied.

When the maximum sustainable axial load is the sought-for quantity, it may be reached when material failure occurs in the extreme fibers of the cross section;

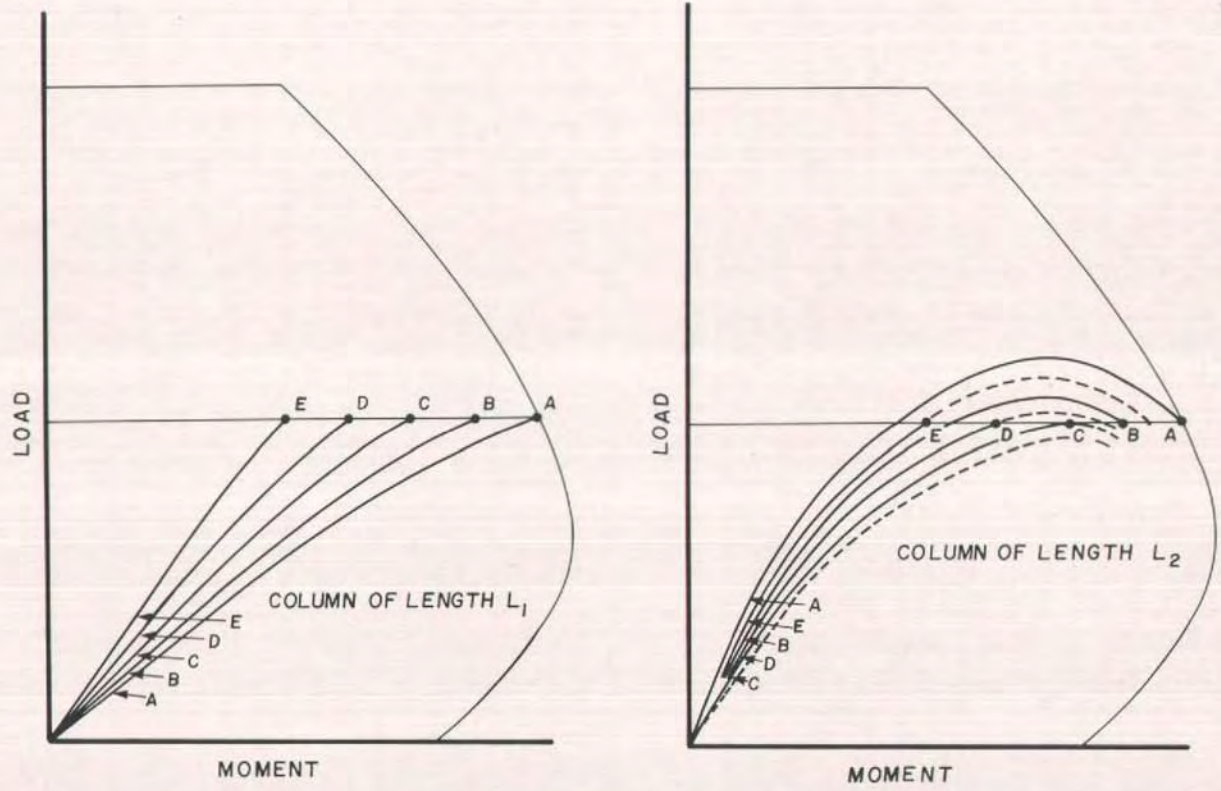

Fig. 13. Possible load paths in load-moment space leading to column deflection curves of Fig. 12.

or it may be reached because at some value of the load the bending moment at a point within the length of the member begins to increase without bound. In practice, this means that:

- If there is no possibility of load shedding, the member would suddenly bow and material failure would occur, although the last calculable value of the moment could be well below the failure value.
- If there is a possibility of load shedding, the axial load on the affected member would begin to decrease, although deflections and interior moments would continue to increase.

For this reason, the search for the maximum sustainable eccentrically applied load, in the basic case of equal end eccentricities and single curvature, is best conducted by the generation of sets of column deflection curves (Ref. 3, p. 273) as shown in Fig. 12. Starting at the midheight of the column, with slope equal to zero and moment equal to that causing material failure (or with the equivalent eccentricity from the thrust line), the column deflection curve is generated by integration of the differential equation as indicated above (Line A, Fig. 12). The starting moment (or eccentricity) at the midheight of the column is then reduced in small steps, and new column deflection curves (Lines B, C, D, E, Fig. 12) are generated.

These curves serve for columns of any length, as shown in the figure; the curve giving the greatest eccentricity at the end of the column is the governing one: either it corresponds to material failure at midheight (Column L_1, Fig. 12) or it corresponds to instability (Column L_2, Fig. 12).

If the load were to be increased at constant end eccentricity corresponding to A, B, C, D, or E in Fig. 12, the midheight cross section would follow load paths such as those shown in Fig. 13. For the column of length L_2, there is simply no equilibrium configuration with load P and eccentricity greater than C. At eccentricity C, the practical column bows sharply to failure at load P (unless the load is reduced as the column deflects under it, to give the descending branch of the load curve).

At higher eccentricity, this unstable behavior is exhibited before the load P can be reached. For the column of length L_1, on the other hand, the eccentricity can be increased to A, whereupon the column cross section fails at load P.

All the column deflection curves of Fig. 12 are at one value of the axial load, and they generate one point on a load-moment interaction curve for each length of column. Repeating the process for different levels of axial load completes the load-moment curves, and allows the identification of maximum end eccentricities (or moments) for any given axial load, for the chosen column lengths.

ESTABLISHING THE *P-M-φ* RELATIONSHIP

Turn now to a more detailed examination of these steps, beginning with the calculation of the moment-curvature relationship. Strictly speaking, this depends upon the exact loading history; if this were known, it would be possible to alter the computational procedure to suit it. However, it is simplest to make the computations as though the axial loads were applied and held constant while the moments or lateral loads are increased to their total or failure values.

This is believed[3] to cause no serious error. For example, as shown in Fig. 14, the points on a beam column loaded monotonically at constant eccentricity would follow Load Paths OA, OB, OC, OD; in the calculations, they are assumed to follow Paths PA, PB, PC, PD, but the final results should be unaffected by this. Had the actual load path not been monotonic (either of the dashed paths), the outcome would have

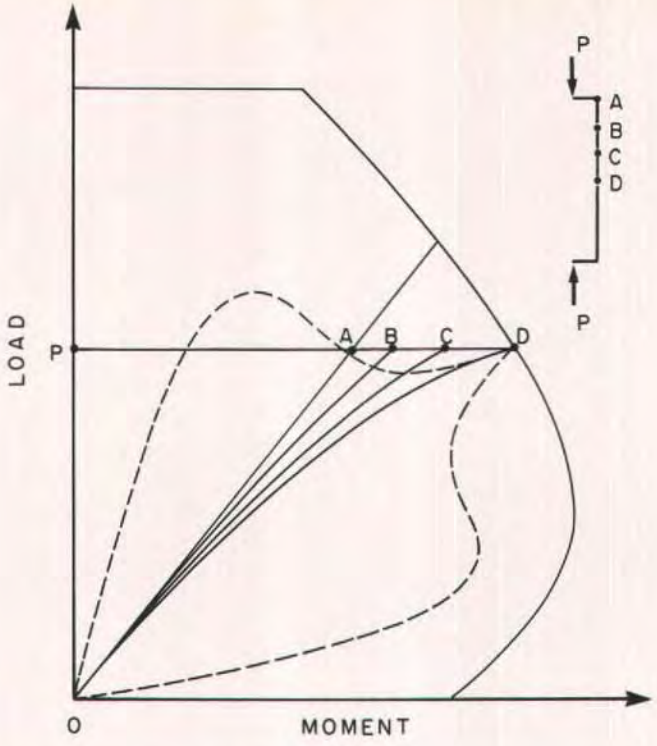

Fig. 14. Load paths in load-moment space.

been influenced, it is believed, in a minor way.

The following additional assumptions are made:

1. Sections originally plane and normal to the neutral surface remain so. There is no twisting or bending out of the plane of loading.
2. The material laws are known and are not path dependent. The fibers in the beam column will obey the stress-strain laws indicated by the chosen uniaxial relationship.

Given particular values of the curvature ϕ and the ordinate of the unstrained fiber y_o, the strain at any point is then defined[18] by:

$$\epsilon = \phi(y - y_o) \tag{13}$$

Or, alternatively, if the curvature and top fiber strain are given:

$$\epsilon = \epsilon_t - (y_t - y)\phi \tag{14}$$

The stress distribution follows from the material law, and the load and moment are given by:[18]

$$P = \int_A \sigma dA = \int_{y_b}^{y_t} b\sigma dy \tag{15}$$

$$M = \int_A \sigma y dA = \int_{y_b}^{y_t} by\sigma dy \tag{16}$$

Since the stress-strain law is generally not known in functional form, the integrations must be carried out numerically. This is easily done by dividing the cross section into narrow horizontal strips, determining the strain and hence the stress at the centroid of each, and evaluating and summing the contribu-

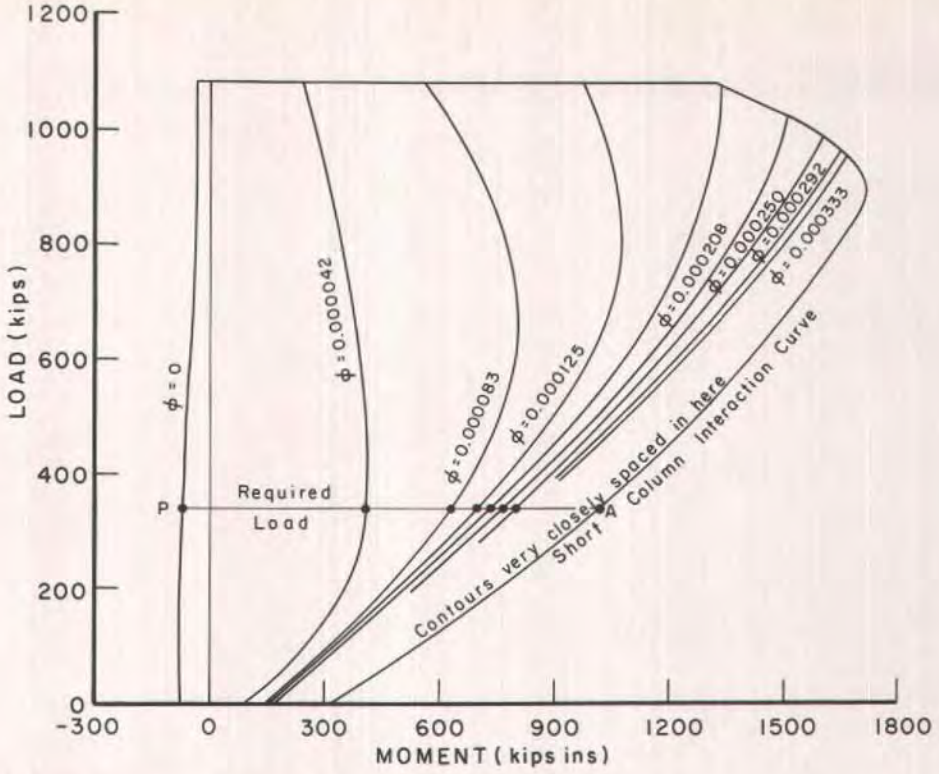

Fig. 15. Curvature contours in load-moment space.

tions of each strip to the load and moment.

Thus, for selected values of the curvature and the ordinates of the unstrained fiber related sets of P-M-ϕ values can be generated. In this way, contours of equal curvature can be developed to cover the entire load-moment space on an interaction diagram for the cross section, as shown in Fig. 15.

Finally, for a selected load path such as PA on Fig. 15 (which corresponds to the moment increasing monotonically from zero at constant load P) the moment-curvature relationship can be obtained by the intersections of the load path with the curvature contours (Fig. 16).

The next step is to solve the differential equation of column equilibrium.

SOLUTION OF THE DIFFERENTIAL EQUATION

Once the moment-curvature relationship for the given load has been established, the differential equation of equilibrium [Eq. (12)] is defined, albeit numerically.

If the displacement $v(x)$ and the slope $v'(x)$ are expanded in Taylor series, one obtains,[19] after truncation:

$$v(x_o + \Delta x) = v(x_o) + \alpha(x_o)\Delta x + 1/2\phi(x_o)\Delta x^2 \quad (17)$$

$$\alpha(x_o + \Delta x) = \alpha(x_o) + \phi(x_o)\Delta x \quad (18)$$

where

$\alpha = v'$, the slope

$\phi = v''$, assumed to be the curvature

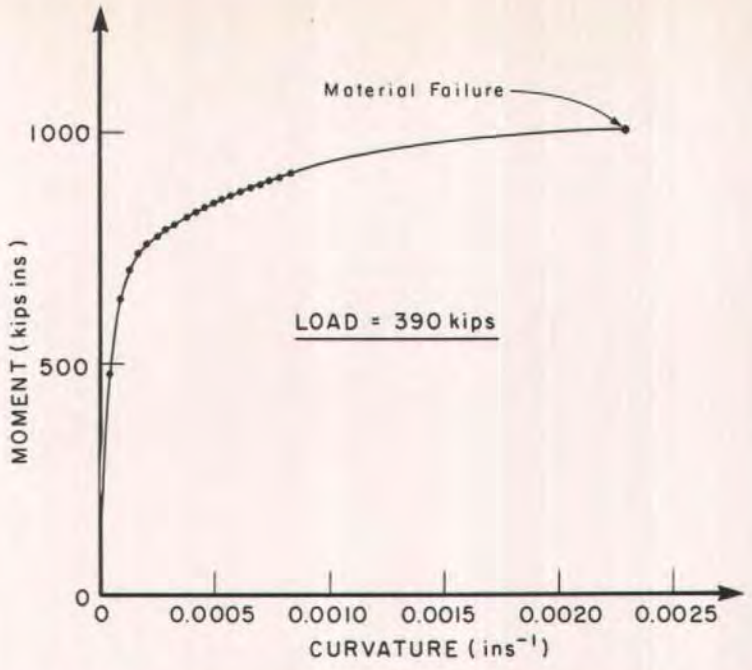

Fig. 16. Moment-curvature relationship for monotonic moment increase at constant load obtained from intersection of load path with curvature contours on Fig. 15.

Note that the truncation of Eqs. (17) and (18) is equivalent to assuming constant or circular curvature between x_o and $x_o + \Delta x_o$; therefore, it is actually more accurate to use ϕ at $x_o + \Delta x/2$ instead of at x_o on the right hand sides of Eqs. (17) and (18).

Now if all the quantities of interest are known or assumed at x_o, Eq. (12) can be used to determine ϕ at the center of the next segment: first evaluate the moment at that point:

$$M = M_o + P\left(v + \frac{\alpha \Delta x}{2}\right) \qquad (19)$$

where

M_o is at $x_o + \Delta x/2$
v and α are at x_o

The curvature ϕ is then obtained from the P-M-ϕ relationship for the given load, and Eqs. (17) and (18) are used to evaluate all the necessary quantities at the next station $x_o + \Delta x$.

Consider the case of a beam column with a given lateral load. Suppose that the maximum possible eccentricity at a given load is to be determined in order to find a point on the load/end moment interaction curve in the presence of the stated lateral load. The eccentricity at $x = L$ is κ times that at $x = 0$. (Other problems, such as the magnified moment for a given lateral load, axial load, and eccentricity are simpler specializations of this case.)

The object is to find the starting eccentricity (at $x = 0$) such that the member is just on the point of failure, either by instability or by material failure. This is done by first seeking an eccentricity so large that the member does fail; it is then reduced in steps of 10 percent until the member does not fail. This establishes the range of values within which the answer lies. This range is then ex-

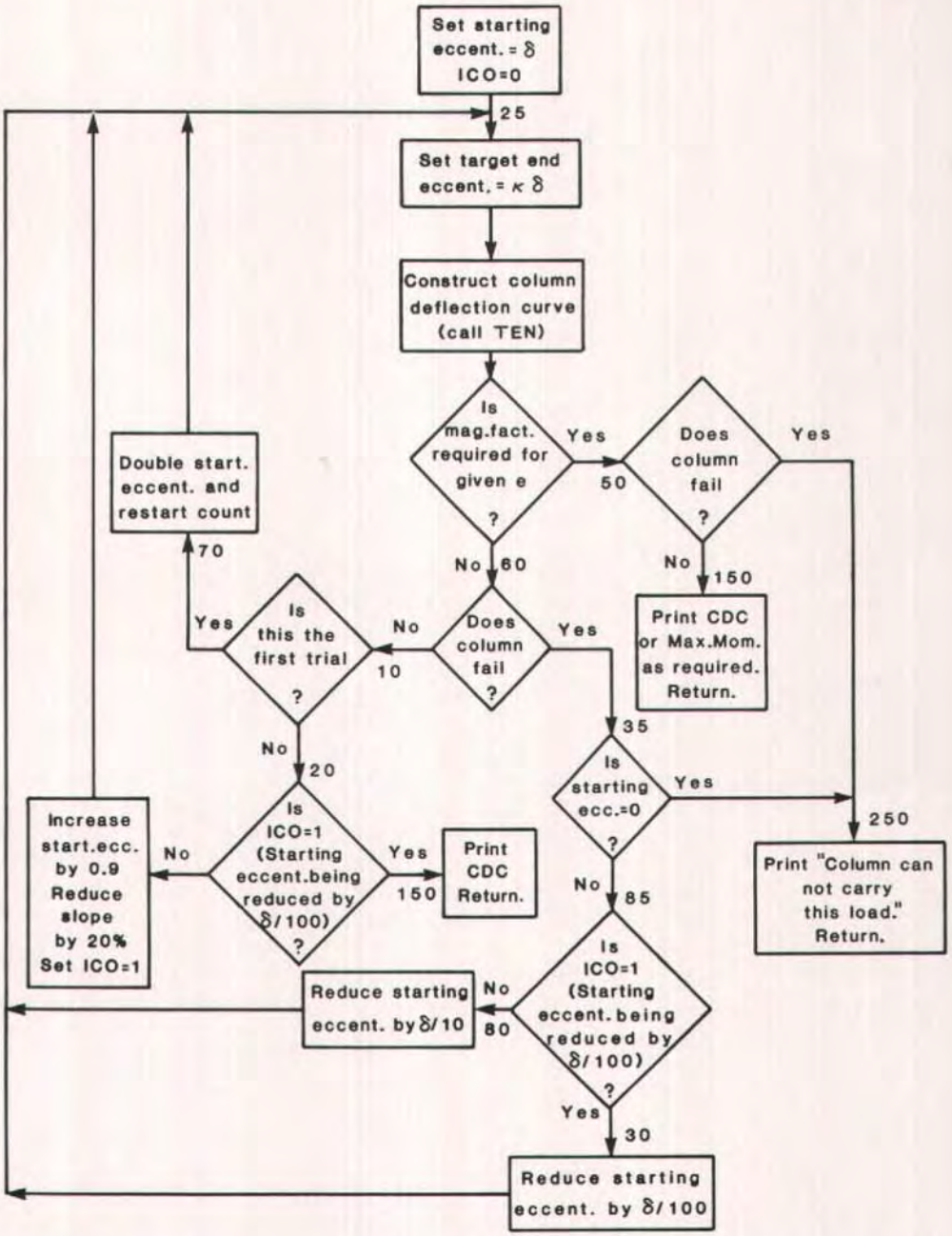

Fig. 17. Flow chart for control of boundary conditions in construction of column deflection curves (Subroutine MSIX).

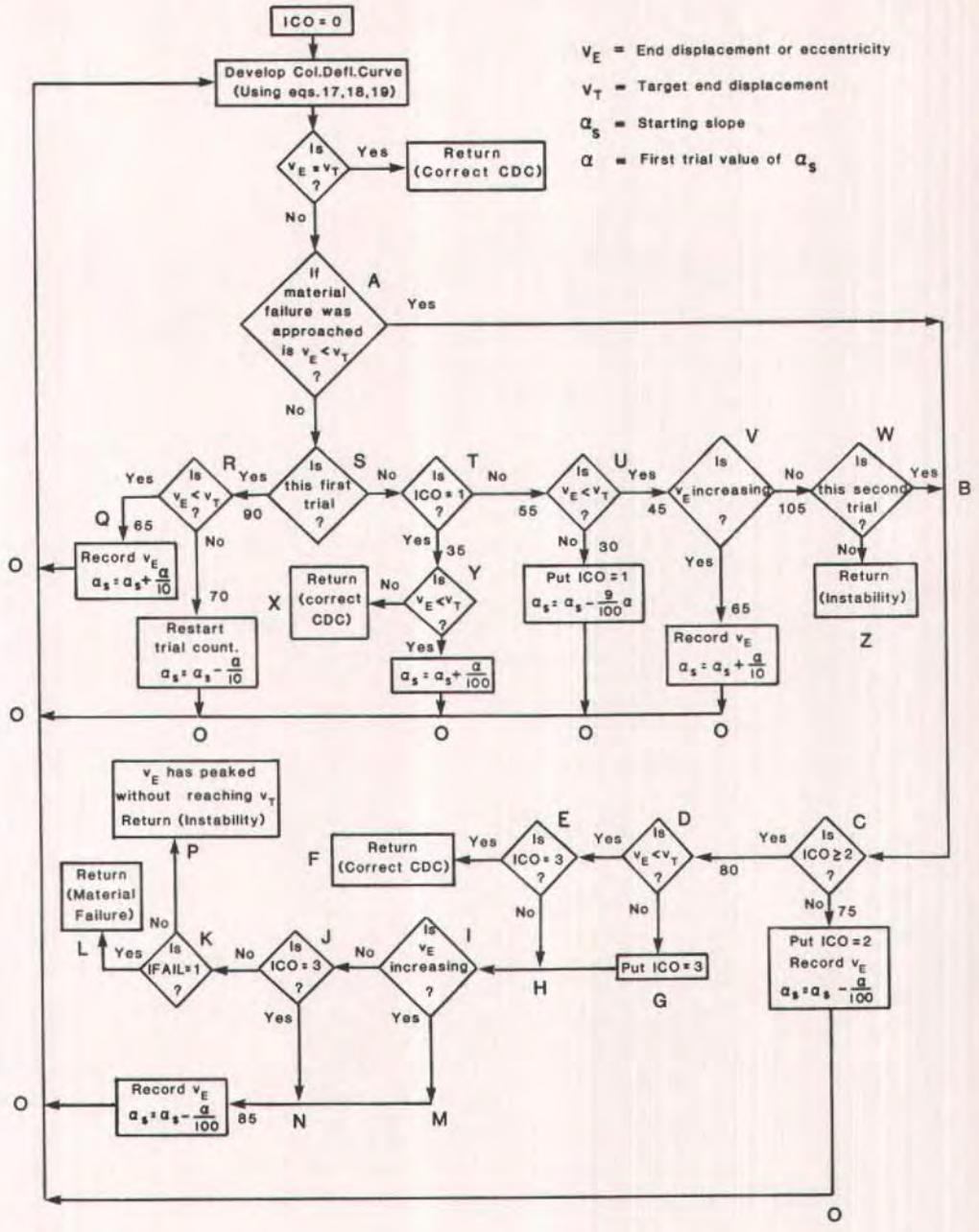

Fig. 18. Flow chart for construction of a column deflection curve (Subroutine TEN). See also Figs. 17 and 19.

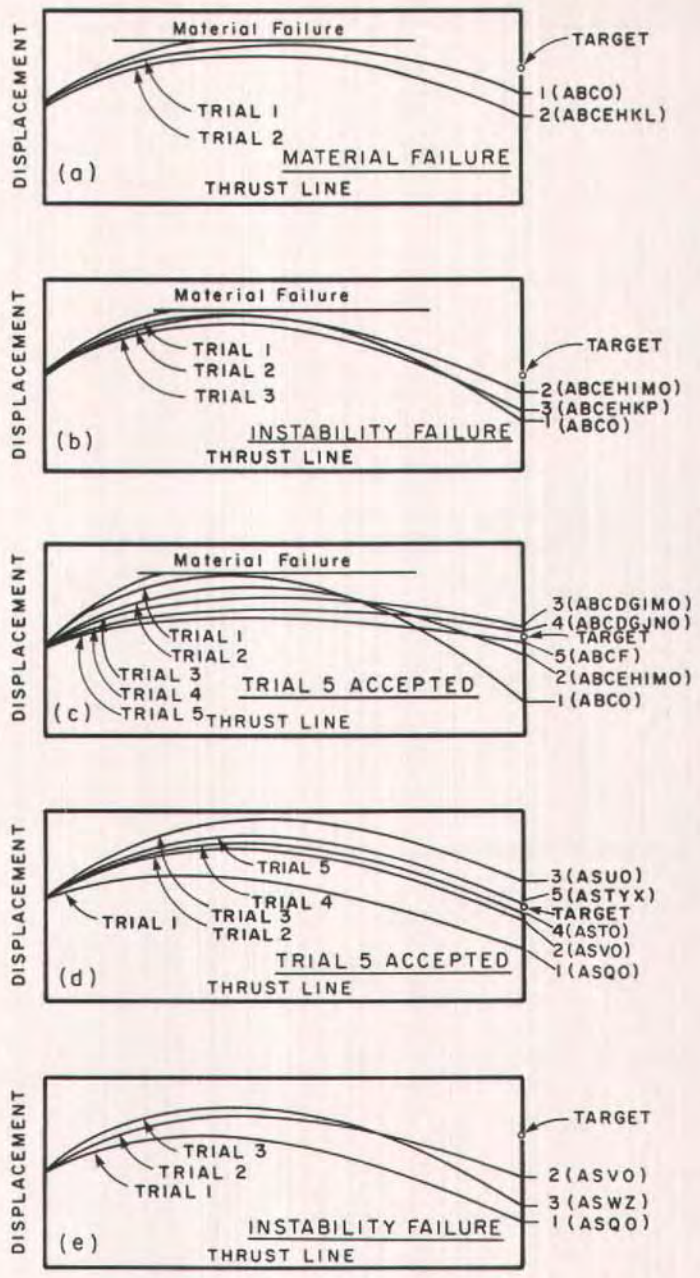

Fig. 19. Examples of construction of column deflection curves, keyed to the flow chart of Fig. 18.

plored in steps of 1 percent of the initial eccentricity until, again, the first value which does not cause failure is found. This is accepted as the answer.

The process is illustrated by the flow chart of Fig. 17, where the node numbers correspond to statement numbers in the program. In each step of this procedure, it was necessary to construct the column deflection curve for the given eccentricities, or to determine that the member failed. This will be discussed in the next paragraph. In the program referred to, it is performed in a subroutine labelled TEN.

Now turn to the problem of constructing the deflection curve for a column with given lateral and axial loads, where the starting and ending eccentricities are fixed. The aim is to vary the starting slope until the correct conditions are reached at the far end. This may not be possible because the bending moment corresponding to failure is reached at some intermediate point, or because, as the starting slope is increased, the eccentricity (or deflection from the thrust line) at the far end approaches the target value and then recedes without reaching it.

This indicates instability failure: no equilibrium position exists having the required eccentricities. The situation is similar to that for the column of length L_2 illustrated in Figs. 12 and 13.

This problem can be handled by the procedure outlined in the flow chart of Fig. 18, which is seen to be fairly complicated. The easiest way to explain it might be to follow through some specific cases, which will be explained in detail below, in conjunction with the flow chart. Before entering into the details, a very brief explanation of each case will be given.

The examples are illustrated in Fig. 19, which shows the deflected shapes of the member. For each case, the axial load, lateral load, and the eccentricity at the left hand end are held constant at the given values, and the slope at the left hand end is varied until the target eccentricity is reached (if possible) at the right hand end.

In Case I (Fig. 19a), the target eccentricity cannot be reached because material failure occurs within the span.

In Case II (Fig. 19b), the eccentricity at the right hand end reaches a maximum short of the target, and then begins to reduce with increasing starting slope (although interior deflections continue to increase). This indicates instability failure.

In Case III (Fig. 19c), two configurations are found giving the correct target eccentricity. The one with the smaller starting slope (and smaller midspan deflection) is the stable one. The other one represents the case where the member has snapped through and is on the descending load branch. Fig. 20 illustrates this case.

In Case IV (Fig. 19d) the starting slope is increased in large steps for Trials 1, 2, and 3. Since Trial 3 overshoots the target, the program returns to Trial 2 and increases the slope in small steps until the target is again reached with Trial 5, which is accepted. Case V is similar to Case II, but the solution is reached by a different path through the flow chart.

These cases will now be described in detail, with an indication of the path followed by the program logic. The reader not interested in the program logic may move to the end of this section.

Case I (see Fig. 19a)

On the first attempt, with a trial starting slope, material failure is reached at some point in the column. The attempt is immediately abandoned, and the starting slope is reduced in small steps until the far end is reached without material failure. The end eccentricity is then below the target value. This may indicate that the target value cannot be reached because of material failure, or

the design may be on a descending branch of the load path; therefore, still smaller values of the starting slope must be tried.

The program is directed along Path ABCO on Fig. 18, to make a second trial with reduced starting slope. On the second trial, the end eccentricity decreases, Path ABCEHKL is followed, and the result is recorded as material failure; the design is on a stable branch of the load path, since increased starting slope leads to increased end eccentricity, but material failure intervenes before the target end eccentricity can be reached.

Case II (see Fig. 19b)

Again, after reducing the slope to avoid material failure, the end eccentricity is below the target value. The program is directed along ABCO as in Case I, but on the second trial with reduced starting slope, the end eccentricity increases (but does not reach the target), indicating that the design is on an unstable load path; the program is directed along ABCEHIMO for a third trial at a further reduced starting slope. This time the end eccentricity also reduces, indicating that the design has moved back along the stable path, reaching the peak before the target, and instability failure (Path ABCEHKP) occurs.

Case III (see Fig. 19c)

The first two trials are exactly as in Case II (Paths ABCO and ABCEHIMO). On the third trial, the end eccentricity again increases and exceeds the target value. The unstable path has to be followed up to the peak, and then down the stable branch until the target is reached. The program is, therefore, directed along Path ABCDGIMO for another trial at a still further reduced starting slope. When the end eccentricity begins to decrease, the process is redirected along ABCDGJNO, until it falls below the target value again, when ABCF is followed, and the result is accepted.

Case IV (see Fig. 19d)

On the first trial, material failure is not encountered, but the far end eccentricity is below the target value (Path ASQO). The starting slope is increased by a large amount and a second trial is made; the far end eccentricity increases, but is still below the target (ASVO). The starting slope is gradually increased until the target is exceeded (ASUO), when one large decrease in the starting slope is made, whereafter it is increased again in small steps. Subsequent trials follow Path ASTO until the target is again exceeded, when Path ASTYX is followed and the result is accepted as correct.

Case V (see Fig. 19e)

The first two trials are as for Case IV (Paths ASQO and ASVO) but eventually, before the target is reached the end eccentricity begins to decrease. Path ASWZ is followed to indicate instability failure.

Case VI

The first trial is as for Case IV (Path ASQO), but on the second trial with a larger starting slope, the end eccentricity decreases. This indicates that the design is on an unstable load path, and Path ASBCO is followed and the process of Case II or Case III is repeated to work back up this unstable load path to the peak and beyond, if necessary.

Other cases can be traced through Fig. 18 in a similar way.

In the special but most common case of columns loaded with equal end eccentricities, causing single curvature but no lateral load, an entirely different procedure is carried out as described in the previous section on the solution of

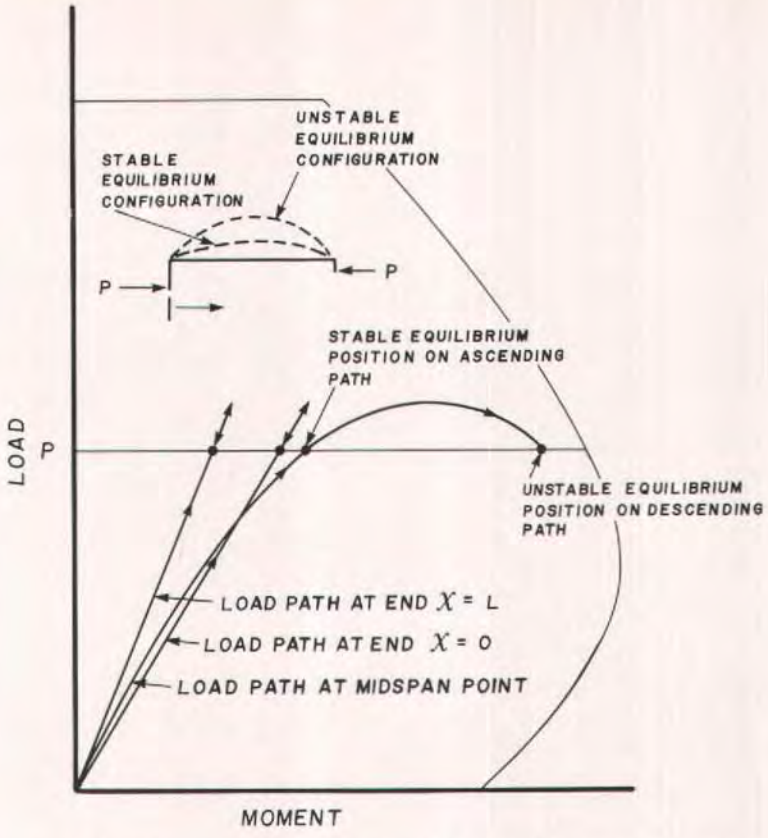

Fig. 20. Load paths at ends and center of eccentrically loaded column, leading to stable and unstable equilibrium configurations.

the differential equations, as shown in Fig. 12. This set of curves allows one to determine the magnification factor for a given eccentricity, or the maximum possible eccentricity (whether governed by instability or material failure) for all lengths of the column for the given load.

APPLICATION OF STRENGTH REDUCTION AND LOAD DURATION FACTORS

In the ACI Code column design, the strength reduction factor is applied at two points in the calculation. It appears first in the moment magnification procedure, where it accounts for the influence of analytical and construction inaccuracies on the Euler load and hence on the moment magnification itself. This is accomplished in the ACI Code method by, in effect, reducing the rigidity EI of the cross section, which is the slope of the moment-curvature relationship.

When the moment-curvature relationship has a "yield plateau," the moment capacity should presumably also be reduced as shown in Fig. 10. It would be subject to variations from the same causes as the rigidity, and its value is now relevant to the moment magnification. The program is written to perform the modifications to the moment-cur-

vature relationship indicated in Fig. 10. The value of ϕ may be entered, or the ACI Code values (with the transition below $P = 0.1\phi A_g f'_c$) may be requested.

The strength reduction factor appears a second time when the magnified moment is compared with the nominal capacity of the member without magnification; the latter is reduced by the capacity reduction factor. This operation is performed by the program; the value of ϕ is entered independently of that used in the magnification procedure. A different value may be used if desired, or again, the ACI Code values may be selected.

The load duration factor β_d is also applied in the ACI Code magnification procedure in such a way as to reduce the rigidity of the cross section by the inverse of $(1 + \beta_d)$. This is again achieved in the program by stretching the curvature axis of the moment-curvature relationship as shown in Fig. 10.

REVIEW OF ASSUMPTIONS

The assumptions made in the foregoing analysis have been stated as they were made, but they will be collected together here for reference:

1. If sway is permitted, the P-Δ moments due to sway have been estimated and the effective length factor is being set at 1 for the effects of column centerline deflection; or the sway-permitted effective length factor, greater than 1, has been estimated to account for both P-Δ moment and centerline deflection.

2. If sway is not permitted, the sway-prevented effective length factor has been estimated or conservatively set at unity.

3. There is no torsional buckling of the section.

4. There is no local buckling of parts of the section, such as the flanges.

5. Deflections are small enough for v'' to represent curvature, so that $EIv'' = M$.

6. Sections originally plane and normal to the neutral surface remain so.

7. The stress-strain laws of the materials are known and are the same in bending as they are in uniaxial stress.

8. The stress-strain laws reflect the duration of loading or other time effects; or the load duration factor β_d correctly models the creep.

9. There is perfect bond between steel and concrete.

10. Material failure of the cross section is due to the concrete reaching some limiting strain.

11. The result is not significantly dependent upon the precise load path in the load-moment space.

Note that Assumption 9 implies that the prestressing tendons and other reinforcement are fully developed at the points of high moment. The reduced capacity of the section in the development region of pretensioned members should be considered separately.

CONCLUSION

The stability analysis of frame structures has been discussed. Generally, the recommended procedure involves a second order elastic analysis (with stiffness modified to account for cracking) to determine the P-Δ effects due to joint translations, followed by magnification of moments based on braced effective lengths to account for centerline deflections.

Prestressed concrete members are more subject to instability rather than to material failure than are conventionally reinforced concrete members; loss of stiffness in column members may therefore be of greater significance in the secondary analysis for P-Δ effects; and the semi-empirical moment magnification procedures need modification, and are in any case less reliable.

However, the large scale production and standardization associated with precast prestressed members suggests the use of computer programs for the mo-

ment magnification solution; in fact, rational analysis is required by codes of practice for the high slenderness ratios often encountered in these members. The preparation of a typical program to perform this task has been discussed, and is described in detail in Appendix B.

The program may be used for the rational analysis of slenderness effects in prestressed and/or reinforced concrete columns, wall panels, or piles. It is useful for developing the load-moment relationships necessary in the design process, with or without slenderness; the solution of particular cases or the preparation of design charts for standardized items may be quite easily and inexpensively carried out.

The difficulty of establishing the effective length for the sway case or, alternatively, of carrying out the second-order analysis for P-Δ effects, remains. Further work is necessary to study the loss of stiffness in prestressed concrete members in the presence of axial load in the inelastic range, and to develop reliable P-Δ analyses when individual members are subject to stability rather than to material failures.

ACKNOWLEDGMENTS

This work was funded by the Natural Sciences and Engineering Research Council of Canada. Computing facilities were made available during the author's sabbatical by the University of the Witwatersrand, Johannesburg, South Africa. Encouragement and help have been received from the PCI Prestressed Concrete Columns Committee, and from other members of the PCI.

* * *

NOTE: Discussion of this paper is invited. Please submit your comments to PCI Headquarters by January 1, 1986.

REFERENCES

1. ACI Committee 318, "Building Code Requirements for Reinforced Concrete (ACI 318-83)," American Concrete Institute, Detroit, Michigan, 1983.
2. MacGregor, J. G., "Stability of Multi-Story Concrete Buildings," ASCE-IABSE Conference on Tall Buildings, Bethlehem, Pennsylvania, SoA-Rep 23-3 Planning and Design of Tall Buildings, V. III, 1972, pp. 517-536.
3. Galambos, T. V., *Structural Members and Frames*, Prentice-Hall, Inc., Englewood Cliffs, N.J., 1968.
4. Wood, B. R., Beaulieu, D., and Adams, P. F., "Column Design by P Delta Method," *Journal of the Structural Division*, ASCE, V. 102, No. ST2, Proceedings Paper 11936, February 1976, pp. 411-427.
5. Lai, S.-M. A., and MacGregor, J. G., "Geometric Non-Linearities in Unbraced Multi-Story Frames," *Journal of the Structural Division*, ASCE, V. 109, No. ST11, November 1983, pp. 2528-2545.
6. Lai, S.-M. A., MacGregor, J. G., and Hellesland, J., "Geometric Non-Linearities in Nonsway Frames," *Journal of the Structural Division*, ASCE, V. 109, No. ST12, December 1983, pp. 2770-85.
7. Kavanagh, T. C., "Effective Length of Framed Columns," *Transactions*, ASCE, V. 127 (1962), Part II, pp. 81-101.
8. Bleich, F., *Buckling Strength of Metal Structures*, Engineering Society Monograph, McGraw-Hill, New York, N.Y., 1952.
9. Johnston, B. G. (Editor), *Guide to Stability Design Criteria for Metal Structures*, 3rd Edition, Column Research Council, John Wiley and Sons, Inc., New York, N.Y., 1976.
10. ACI Committee 318, "Commentary on Building Code Requirements for Reinforced Concrete (ACI 318-83)," American Concrete Institute, Detroit, Michigan, 1983.
11. Chu, K. H., and Chow, H. L., "Effective Column Length in Unsymmetrical Frames," Publication, International Association of Bridge and Structural Engineering (IABSE), V. 29-1, 1969.
12. MacGregor, J. G., and Hage, S. E., "Stability Analysis and Design of Concrete Frames," *Journal of the Structural Division*, ASCE, V. 103, No. ST10, Proceedings Paper 13280, October 1977, pp. 1953-1970.
13. Nixon, D., Beaulieu, D., and Adams, P. F., "Simplified Second-Order Frame Analysis," *Canadian Journal of Civil Engineering*, V. 2, No. 4, December 1975, pp. 602-605.
14. Rosenblueth, E., "Slenderness Effects in Buildings," *Journal of the Structural Division*, ASCE, V. 91, No. ST1, February 1965, pp. 229-252.
15. Nathan, N. D., "Slenderness of Prestressed Concrete Columns," PCI JOURNAL, V. 28, No. 2, March-April 1983, pp. 50-77.
16. Gere, J. M., and Weaver, W., *Analysis of Framed Structures*, Van Nostrand, Co. Inc., Princeton, New Jersey, 1965, pp. 428-431.
17. Ghali, A., and Neville, A. M., *Structural Analysis*, Chapman and Hall, London, 1977, Chapter 15.
18. Timoshenko, S. P., and Gere, J. M., *Theory of Elastic Stability*, Second Edition, McGraw-Hill, New York, N.Y., 1961.
19. Nathan, N. D., "Slenderness of Prestressed Concrete Beam-Columns," PCI JOURNAL, V. 17, No. 6, November-December 1972, pp. 45-57.
20. Salmons, J. R., and McLaughlin, D. G., "Design Charts for Proportioning Rectangular Prestressed Concrete Columns," PCI JOURNAL, V. 27, No. 1, January-February 1982, pp. 120-143.
21. Wang, P. T., Shah, S. P., and Naaman, A. E., "Stress-Strain Curves of Normal and Lightweight Concrete in Compression," PCI JOURNAL, V. 75, No. 11, November 1978, pp. 603-611.
22. Rüsch, H., "Researches Towards a General Flexural Theory for Structural Concrete," *ACI Journal*, V. 32, No. 1, July 1960, pp. 1-28.
23. Sheppard, David A., "Seismic Design of Prestressed Concrete Pilings," PCI JOURNAL, V. 28, No. 2, March-April 1983, pp. 29-49.

* * *

APPENDIX A — NOTATION

A = cross section area
b = width of cross section at ordinate y
C_m = modifier to magnification factor for unequal end eccentricities
E = Young's modulus
E_c = E of concrete
h = story height
H = lateral force
I_c = moment of inertia of concrete cross section
k = effective length factor
K = lateral stiffness of frame
L = unbraced length
M = moment
M_o = primary moment
M_{2b} = larger factored end moment (braced case)
M_{2s} = larger factored end moment (sway case)
M_c = magnified column moment
M_{ext} = external moment
M_{int} = internal moment
P = axial load
P_o = maximum pure axial load
P_c = critical load
P_E = Euler load
P_u = ultimate load
r = radius of gyration
v = transverse deflection of member centerline
x = distance along member centerline
y = ordinate of point in cross section
y_o = ordinate of unstrained fiber
y_b = ordinate of bottom fiber
y_t = ordinate of top fiber
α = slope of column deflection curve
α = angle between imaginary bracing and horizontal
β_d = ratio of maximum factored dead load moment to maximum factored total load moment (always positive); the load duration factor
γ = flexibility factor [see Eq. (3)]
δ = magnification factor
δ_b = magnification factor (braced case)
δ_s = magnification factor (sway case)
δ = first trial value of starting eccentricity
Δ = deflection of joint normal to axis of beam column
Δ_1 = Δ calculated by first order analysis
Δ_2 = Δ including secondary effects
ϵ = strain
ϵ_t = strain in top fibers
η = factor used in calculation of P_c [Eq. (11)]
θ = factor used in calculation of P_c [Eq. (11)]
κ = ratio of eccentricity at bottom to eccentricity at top
λ = factor used in calculation of P_c [Eq. (11)]
σ = stress
ϕ = curvature
ϕ = strength reduction factor

* * *

APPENDIX B — A COMPUTER PROGRAM FOR RATIONAL ANALYSIS OF BEAM COLUMNS

What follows is a detailed description of a computer program to perform the analysis described in the paper. It was written by an unsophisticated programmer with the intention of making it easy to understand and to modify rather than to make it efficient from a computational viewpoint; running costs are generally not a large factor. Because it was intended to be used for research purposes, the program as presented here is capable of handling a variety of cases and all the computed curves are generated from an extremely dense array of points.

For practical purposes, the scope could be more limited and the arrays could be reduced in size. It is hoped that the processes of familiarization, adaptation, and modification have been made as easy as possible. The assumptions and theories used are as set forth in the paper.

Equations referred to by number in this Appendix are those in the paper. A listing of the FORTRAN source program is available at cost of reproduction from PCI Headquarters.

Capabilities

The problem to be solved is illustrated in Fig. B1. The cross section may have any polygonal shape (or any curved shape which can be adequately approximated by a polygon) with any arrangement of prestressing tendons and/or nonprestressed reinforcing bars.

The axial load P can be applied at any eccentricity e at one end, and at any eccentricity κe at the other. Note that κ may be positive, negative, or zero. Initial crookedness in the shape of a sine curve is provided for: the amplitude must be supplied by the user. Camber due to prestress is automatically accounted for. The primary bending moment due to lateral loads may have any shape; it is entered by means of its tenth point values.

For given values of P, e, κ, and primary moment, the maximum value of the magnified moment within the span can be computed; or, while the other parameters are held constant, the eccentricity e can be increased until failure.

Failure may be due to material failure at some interior section where the magnified moment reaches the short column capacity, as for the load P_1 applied at eccentricity e_1, or due to instability, as for the load P_2 applied at eccentricity e_2 (Fig. B1). The output will indicate which has occurred.

By entering several loads and generating several points such as A_1, A_2, one can develop the line through them, which is an interaction curve of load P versus end moment Pe for a given slenderness ratio.

The program can also be used merely to compute the short column interaction curve for complex cross sections, or the moment-curvature relationships at given loads. In this mode it generates design information such as that given by Salmons and McLaughlin,[20] for any shape of member with any arrangement of reinforcement and prestressing tendons. Length effects can be included by running the whole program.

General Procedure

The behavior of the section as the strain is uniformly increased to failure is first established. This is the load-moment relationship at zero curvature; it may lie along the zero moment load axis, but only for symmetrically reinforced sections (Fig. B2). In fact, it is the moment necessary to remove the camber due to prestress in the presence of the given axial load.

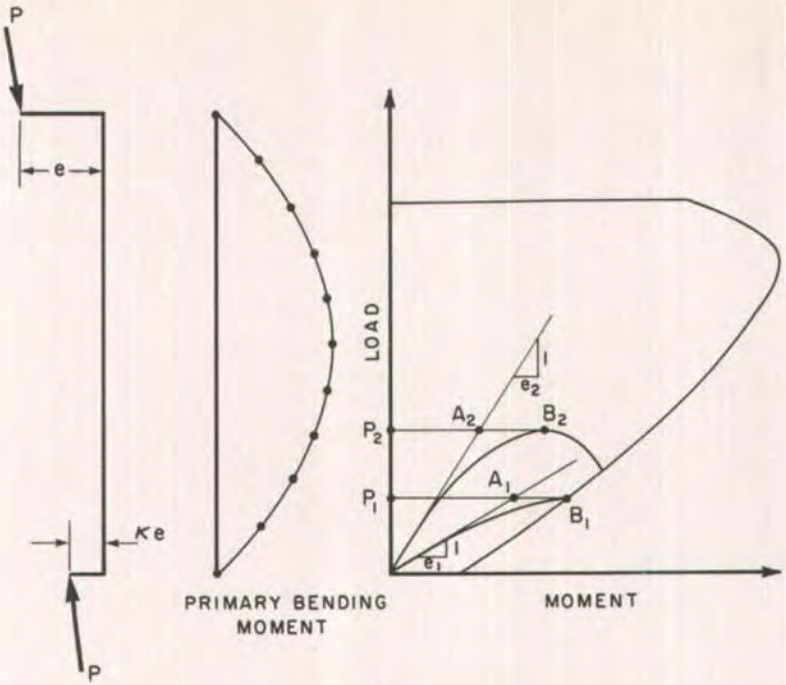

Fig. B1. Definition of the problem to be solved.

Then the load-moment curve for the short column corresponding to the maximum concrete strain is calculated, together with the associated curvatures (Fig. B2). These values are used to determine the range of curvatures and moments which will be encountered with the particular section under investigation.

A set of intermediate curvatures is then selected and contours of equal curvature are calculated, covering the entire feasible area of the load-moment diagram. For each of the desired loads, values of moment and curvature are obtained from the intersection of the load coordinate with these contours, establishing the moment-curvature relationship for that load (Figs. 15, 16 of the main part of the paper).

This moment-curvature relationship is then used to obtain the column deflection curve for the given load and boundary conditions by a numerical procedure.

Each of these steps is performed in a separate subroutine named MONE, MTWO, MTHREE, etc., which are called by a short control program. Various arithmetic procedures which are repeatedly used by these main subroutines are executed in another set of subroutines named ONE, TWO, etc. The results are printed out by a set of routines named WRITE1, WRITE2, etc., any of which can be suppressed if only specified data are required. The input data, from Subroutine INPUT, are shared by the main subroutines in common statements, but the computed values are generally transferred in the calling statements for the subroutines. All input data referring to the material laws are grouped in a separate common statement.

Detailed descriptions will now be

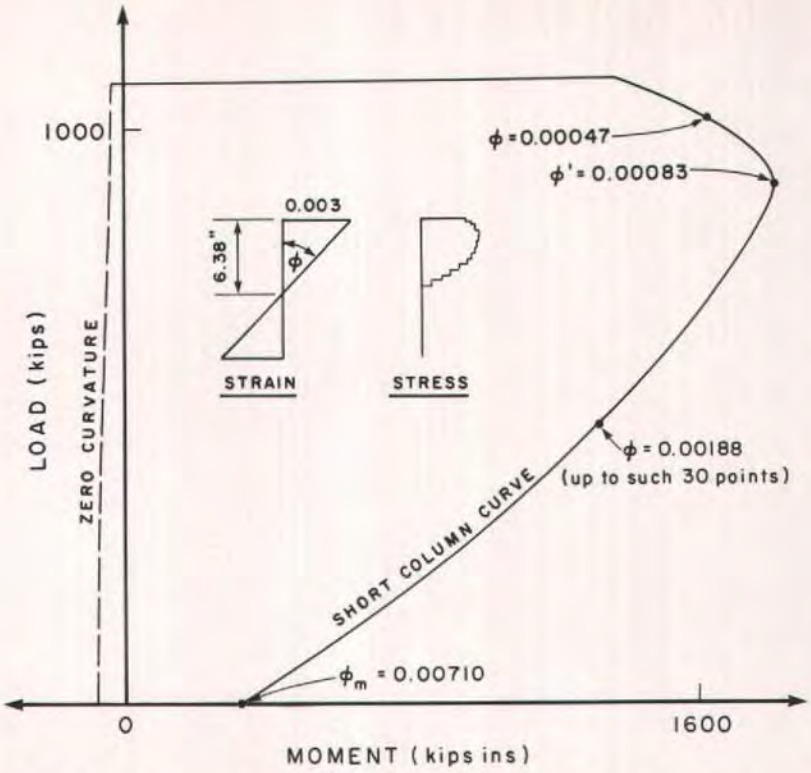

Fig. B2. Short column load-moment relationship with curvatures on boundary of load-moment space, for the section of Fig. B3.

given of each of these routines, illustrated by means of the actual output from the section of Fig. B3.

MAIN Program

The principal variable names are listed in comment statements. The subroutines to carry out the steps described above are called in turn, each followed by the appropriate output routine. Provision is made for stopping after generation of the short column data, or after the moment-curvature relationships. Any of the output segments may also be suppressed.

INPUT

Details may be found in the program documentation; this section will provide a general description of the options open to the user.

The coordinates of the concrete cross section are entered with respect to a set of axes set up so that the neutral axis will be parallel to the x-axis. The origin should be set outside the section, so that the entire section lies in the first (positive) quadrant. Any polygonal shape may be entered, with up to 20 sides. Thus a circular section can be approximated by a twenty-sided polygon, if required.

Data for material laws will be discussed below. Arrays are dimensioned for up to 20 nonprestressed bars which may have different areas and coordinates. (Since plane sections are assumed to remain plane and the neutral axis is to

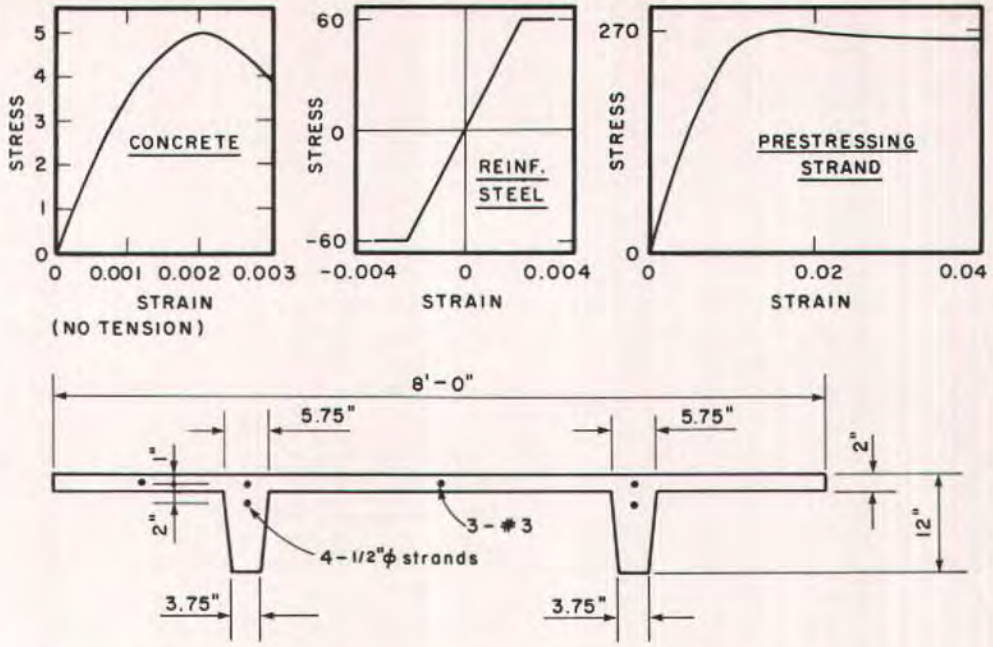

Fig. B3. Illustrative example: double tee used as loadbearing wall unit.

be parallel to the x-axis, the x-coordinate of bars is actually immaterial, and bars with a common y-coordinate might well be lumped together.) At present, these bars must all have the same material law.

Up to 20 prestressing tendons can be included, with different areas, centroids, and prestress forces. The prestress can be entered in the form of a stress, a force, or a strain, corresponding to zero strain in the surrounding concrete, i.e., the value of stress, strain, or force must be that existing after all losses except elastic shortening. Again, x-coordinates are immaterial and tendons with equal y-coordinates can be lumped; and, again, all tendons must have the same material law.

Up to 20 axial loads may be investigated; they may be entered as absolute values or as ratios of the maximum axial load. Up to 20 column lengths can be studied. If there is lateral loading, the primary bending moment must be entered for each length by giving the values at the tenth points and the two ends. The amplitude of the initial crookedness (assumed to be a sine curve) must be entered for each length, if desired.

MONE

This is a subroutine to determine the area and centroid of the concrete section, and the maximum load. The load-moment relationship for zero curvature is also computed; this will be a straight line coinciding with the load axis on the load-moment diagram for symmetric sections. But, if the reinforcement is not symmetrically placed with respect to the plastic centroid,* it may be a curving line. The data generated by this subrou-

*The centroid of forces when a uniform strain corresponding to the peak concrete stress is applied to the entire cross section.

tine are not necessary for the final result, but they are used in the program for selecting other parameters.

The area and centroid of the concrete are calculated in Subroutine FIVE, and the prestressing is converted to strain if it was given in some other form. The strain in the concrete is then uniformly increased in 30 steps from zero to failure, while compatibility is maintained with the steel elements. The load and moment corresponding to each step are calculated, defining 30 points on the load-moment-zero curvature relationship (see Fig. B2).

MTWO

This is a subroutine to determine the load-moment-curvature interaction curve for the nominal load capacity of the short column.

The depth of the section is calculated and divided into 30 parts. The neutral axis is then placed at each of these positions in turn, with the extreme fiber strain of the concrete set to equal the value defined as failure. The total force and moment resulting from stresses on the concrete section are calculated in Subroutine THREE, using Eqs. (15) and (16).

The compatible strains in the steel elements are computed, and the corresponding stresses, from Subroutine SIX, used to obtain the forces which are included in the total force and moment. The curvature is calculated by dividing the failure strain in the concrete by the neutral axis depth [Eq. (13)]. See Fig. B2.

MTHREE

This is a subroutine to calculate contours of equal curvature covering the load-moment diagram.

The curvature ϕ_m at zero load is extracted from the data generated by MTWO; this is the maximum curvature. The value of curvature ϕ' at the balanced load and moment is also determined. If $\phi_m > 2\ \phi'$, the interval between ϕ' and ϕ_m is divided into 10 parts and the interval between 0 and ϕ' is divided into 20 parts. If $\phi_m \leq 2\ \phi'$, the interval from 0 to ϕ_m is divided into 30 parts. These divisions define the curvature values for which contours will be developed; the procedure is found to give a reasonable coverage of the load-moment diagram (see Fig. B2). For practical purposes, the number of contours could be greatly reduced.

A contour of equal curvature is then generated for each of these curvatures. The extreme fiber strain is set equal to the failure value for the concrete, and the neutral axis depth is set to give the desired curvature (curvature = extreme fiber strain/neutral axis depth). Subsequently, the neutral axis depth is decreased in steps of $\frac{1}{30}$ of the member depth, while the curvature is kept constant. For each neutral axis depth the force and moment arising from the concrete stresses are calculated by Subroutine THREE.

The compatible strains and hence the stresses in the steel elements are then computed, and their contributions are added to the load and moment values. Thus, up to 30 pairs of values of load and moment are computed to define each of 30 contours of equal curvature. See Fig. 15 of the paper. The number of pairs of values could also be reduced for practical purposes.

MFOUR

This is a subroutine to develop moment-curvature relationships for the given loads. For each of the curvature contours obtained in MTHREE, a value of moment is interpolated (by means of Subroutine SEVEN) at each of the given loads. On the zero curvature relationship, the value of moment at zero curvature for the given load is interpolated, and the maximum moment and the corresponding curvature are obtained by

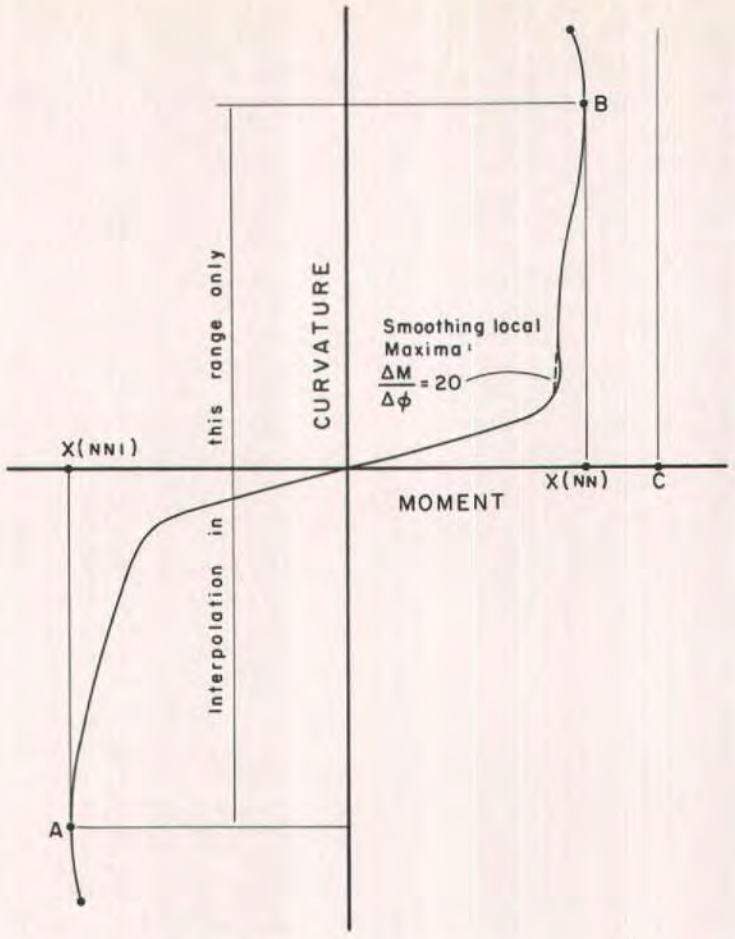

Fig. B4. Interpolation for curvature as a function of moment.

interpolation on the short column relationships. Thus up to 32 pairs of values of moment and curvature are obtained for each load, defining the moment-curvature relationship for that load.

Generally, the moment increases monotonically with curvature up to failure, or up to some maximum, whereafter there is a steadily descending branch to material failure (see Fig. B4). When interpolation is made to find the curvature for a given moment, the interpolation routines automatically reject the descending branch of the curve; interpolation is made only on the ascending branch and the maximum moment represents failure.

Occasionally, for example with I-shaped sections where tension is allowed in the concrete and there is very little reinforcement, there may be a local maximum moment before the overall maximum is reached. This also is shown on Fig. B4. In that case, to avoid problems with the interpolation routine, the curve is smoothed by removal of the first, local maximum, as shown in Fig. B4. This is slightly conservative, but is

believed to deviate very little from the true final result.

If there is to be reverse curvature (i.e., if the end eccentricities are such as to produce double curvature) the moment-curvature relationship must be extended into the negative range. If the cross section is symmetric about an x-axis, the extended portion of the curve is merely the mirror image of the portion already calculated. Subroutine NINE is used to carry out this operation.

If the cross section is not symmetric about an x-axis, Subroutine EIGHT is used to reverse all the coordinates (i.e., to turn the section upside down, as it were) and the complete process, involving Routines MTWO, MTHREE, and MFOUR, is repeated. Subroutine EIGHT is again used to merge the positive and negative moment-curvature relationships.

MFIVE

This routine deals with the special case where there is no lateral load but equal end eccentricities, and the maximum eccentricity is required at given load levels.

The procedure consists of starting at midheight of the column, with the maximum possible moment at that point. This maximum moment is obtained from the high point on the moment-curvature relationship for the given load. At the midheight point, the starting slope is zero, and the deflection (measured from the thrust line) is given by the starting moment divided by the load.

The column deflection curve is now constructed using Eqs. (17), (18), and (19). This process is continued, as described in the paper, until a complete quarter wave of the column deflection curve has been generated, or until the half lengths of all the columns to be investigated have been exceeded. The end deflections of all the columns are noted. (See Fig. 12 in the paper.)

Returning to midheight, the starting moment and therefore deflection are reduced by a small amount chosen by the user (the default value is 0.05 times the maximum moment) and another column deflection curve is generated. The process is repeated until the end deflection is decreasing for all lengths; the maximum end deflection is the required value: the end eccentricity to cause failure. If it was obtained from the first column deflection curve, which started with the maximum moment at midheight, it represents material failure; if it was obtained from a subsequent curve with lower midheight moment, it represents instability failure.

MSIX

This routine develops the column deflection curves for the more general case in which the end eccentricities are not equal and there is applied lateral load. In contrast to MFIVE, each length case must be handled separately, since the column deflection curves are constructed from the end rather than from the midheight, as described in the paper under "solution of the differential equation."

The segment length is first adjusted if necessary so that there will be an exact number of segments. Then the starting slope and deflection (or eccentricity) are selected. The problem is to determine the order of magnitude of slope and deflection appropriate to the column under study, since these may vary widely from case to case.

The approximate initial slope of the moment-curvature relationship is determined by dividing the fifth positive value of the moment by the corresponding curvature. This gives the initial EI value. Now, the slope at the end of a simply supported beam carrying a uniform load is $ML^2/(3EI)$, where M is the maximum moment.

Therefore, the order of magnitude of the slope in a given column is expected to be:

$$\alpha = \frac{M_c L^2}{5EI}$$

where

M_c = maximum moment capacity of cross section

EI = initial value of EI as determined above

The first starting value of the slope is set equal to α.

The initial eccentricity is set equal to:

$$\delta = \frac{M_c - M_p}{P}$$

where M_p is the maximum value of the primary moment.

Increments of the starting eccentricity are first set to $\delta/10$, and then to $\delta/100$ for fine adjustments. If the program is being used to find the magnification factor for a given eccentricity, of course, the initial value is set to that quantity and no incrementation is required.

The procedure to be followed from this point requires the establishment of a starting eccentricity which will lead to failure. Thus, with the initial value set to δ as defined above, a column deflection curve is calculated by the Subroutine TEN.

If the column does not fail, subsequent trials are made with 2δ, 4δ, etc., until failure is achieved. The starting value is then reduced in steps of $\delta/10$ until failure does not occur. At that stage the last step is retraced, with the initial eccentricity now being reduced in steps of $\delta/100$, until failure again does not occur; this last trial is taken to give the configuration of the column which is "just safe."

The starting slope is set to α, as defined above, when TEN is called for the first time. After that, it is left equal to the value returned from TEN, except when the last step in eccentricity is about to be retraced, when it is reduced by 20 percent.

Fig. 17 of the paper shows the partial flow chart for MSIX.

ONE

In the numerical integration of stresses over the concrete area, the latter is divided into narrow strips parallel to the neutral axis, and this subroutine is used to define the extent of such a strip. (A constant stress will then be assumed over each strip.)

Given the coordinates of the apices of a polygon, and the y-coordinates defining the upper and lower boundaries of the intersecting strip, the subroutine will determine the coordinates of the sub-polygon which lies within the strip. (If the whole of the original area lies within the strip, the original corner coordinates will be returned.)

The end points of each side of the given polygon are examined in turn; it is established whether the side being examined lies wholly outside or wholly inside the intersecting strip, or whether it is entering or leaving that space. Subroutine TWO is then used to evaluate the coordinates of the point where a line actually crosses one of the strip boundaries. The corners of the new sub-polygon consist of these points together with the original ones which lay within the strip.

TWO

This short subroutine determines the coordinates of the point at which a given line crosses a line of constant y.

THREE

This subroutine is used to integrate the concrete stresses to give the total force and moment. The coordinates of the corners of the concrete area and the y-coordinate of the neutral axis are given. The strain distribution is implicitly given, either in the form of the extreme fiber strain or as the curvature (equal to the extreme fiber strain divided by the neutral axis depth). The areas above and below the neutral axis are each divided into 20 strips of equal

depth, parallel to the neutral axis. (If the material law for the concrete is from 1 to 4, it is assumed that tension is not allowed and the area below the neutral axis is not considered.)

Each of the 40 strips is considered in turn; the coordinates of the corners are found using ONE, and the area and centroid of each strip are found using FIVE. The material law is then used in SIX to determine the stress at the centroid and the force in the strip (assuming it is uniformly stressed) and its moment about $Y = 0$ are calculated.

FOUR

This is a short subroutine to determine the biggest and smallest of a list of numbers. It is used, for example, in finding the overall depth of a cross section.

FIVE

This is a subroutine to find the area and centroid of a polygon with n apices defined by coordinates x and y. They are given by:

$$\text{Area} = \tfrac{1}{2} \sum_{i=1}^{n} y_i (x_{i+1} - x_{i-1})$$

Moment of area (about $y = 0$) =

$$\tfrac{1}{6} \sum_{i=1}^{n} (x_{i+1} - x_i)(y_{i+1}^2 + y_{i+1} y_i + y_i^2)$$

The apices are taken in cyclic order in either direction.

SIX

This redirects the program to the appropriate subroutine for the assumed material law, which is defined by the parameter MATLAW. The routines MAT1, MAT2, etc., then determine the stress corresponding to the given strain or vice versa. (The sought-for quantity is set to zero in the calling program.)

MAT1 interpolates in a curve defined by pairs of points entered with the input. It is assumed that there is no tensile stress. The routine is intended to represent concrete.

MAT2 represents the stress-strain law of concrete in the functional form:

$$f_c = \frac{2\,(\epsilon/\epsilon_o) f_c'}{1 + (\epsilon/\epsilon_o)^2}$$

where

f_c' = cylinder strength

ϵ = strain

ϵ_o = strain at peak stress

Again, it is assumed that there is no tensile stress.

MAT3 contains stored pairs of stress-strain values representing points on an experimental curve taken from the literature.[21] It is entered with the peak stress and the corresponding strain for the case being considered, and the stored values of stress and strain are scaled up or down to pass through this point. The current stress or strain is found by interpolation. This curve seems more appropriate for very high concrete strengths (about 7 ksi).

MAT4 gives the stress-strain law in the functional form proposed in Ref. 21.

MAT5 is similar to MAT1. It is intended for steel, and tension may be permitted.

MAT6 is a bilinear stress-strain curve for the elastic/perfectly plastic case. It is intended for mild steel, and the Young's modulus and yield stress must be entered with the data.

MAT7 is similar to MAT5. It is intended for prestressing steel.

MAT8 contains stored pairs of stress-strain values for a typical seven-wire strand with $f_{su} = 270$ ksi. If it is entered with a value of f_{su} other than 270, all the stress values are scaled up or down appropriately.

MAT9 uses the trilinear stress-strain law defined in the British Code of Practice CP110 for steel reinforcement. It

must be entered with the yield stress in MPa.

MAT10 is similar to MAT1, with tension allowed. It is intended for use with concrete where MAT5 and MAT7 are used for mild and prestressed steel.

MAT11 is similar to MAT3, using a curve taken from Ref. 22. It appears to be more appropriate for the usual concrete strengths, up to 5 or 6 ksi.

Other stress-strain laws can easily be entered as MAT11, MAT12, etc.

SEVEN

This subroutine contains a linear interpolation procedure which is used repeatedly throughout the computations for finding values of stress in terms of strain, curvature in terms of moment, etc. Cubic interpolation has been used for research purposes, but the difference in the end result appears to be neglible.

Several points defining the relationship between x and y are given. The routine first investigates the relationship to determine the range over which it is single valued in y, i.e., the number of points for which x is increasing; the remaining points are discarded (see Fig. B4).

The position of the point $\bar{x}$ for which $\bar{y}$ is desired is determined. $\bar{y}$ is calculated by linear interpolation. If $\bar{x}$ lies outside the range of x, the value of $\bar{y}$ is linearly extrapolated from the last two points and a message is printed to that effect. If $\bar{x}$ has a value that cannot be reached by x, such as C on Fig. B4, the value of y corresponding to the nearest valid x value, such as that at B, is given, and an appropriate message is printed. This may indicate a serious error, or it may only be that the round off error has led to the value of $\bar{x}$ (NN) being slightly overestimated.

EIGHT

This subroutine is used when double curvature is present in unsymmetrical sections. The previously generated positive branch of the moment-curvature relationship is stored in a temporary location and the section is then inverted. All the relevant coordinates are transformed to read from a new origin on the opposite side of the neutral axis. The program then returns to calculate a new moment-curvature relation, which will be the negative branch.

NINE

This subroutine merges the positive and negative branches of the moment-curvature relationships when double curvature is present. In the unsymmetric case, both branches have been calculated, and it is a matter of retrieving the positive branch from temporary storage and of merging the two. In the symmetric case, the negative branch is constructed as the mirror image of the positive branch.

TEN

The column deflection curve for the general case is computed here, when this subroutine is called by MSIX. The starting eccentricity (Deflection DEFL(1) measured from the thrust line) and the target eccentricity at the other end, as well as the starting slope for the first trial, are given by MSIX. The object is to vary the starting slope until the target eccentricity at the other end is reached.

This may not be possible because the bending moment corresponding to failure is reached at some intermediate point, or because, as the starting slope is varied, the eccentricity at the far end approaches and then recedes from the target value without reaching it. This signifies instability failure.

Starting with the values obtained from MSIX, the column deflection curve is computed node by node as described for MFIVE, except that the bending moment now contains a contribution

from the primary moment, obtained by interpolation.

The starting slope is increased in steps of $\alpha/10$ (after an initial reduction, if required, because of material failure within the span) until the end deflection exceeds the target value. The subroutine then retreats to the previous starting slope and increases it in steps of $\alpha/100$ until the end deflection again exceeds the starting value. This is taken to be the correct value.

If the end deflection approaches the target and then recedes without reaching it, while the starting slope is continuously increased, this signifies instability failure. If the end deflection immediately begins to decrease as the starting slope is increased, this means the member is in an unstable configuration, representing post-buckling behavior; the starting slope is then continuously reduced by $\alpha/100$ until the end deflection begins to reduce also. If, at this stage, the end deflection is less than the target, instability failure is present. If the end deflection is greater than the target, the starting slope is gradually reduced until the target is reached from above, indicating a stable equilibrium configuration.

If, during the construction of a column deflection curve, the moment at an interior node reaches the maximum value, corresponding to material failure, there is an immediate return to the start, with the starting slope reduced by $\alpha/100$. This is repeated until the end is reached without attaining the failure moment. If the end deflection is then below the target value, it means the target cannot be reached, and material failure is present unless this was the first trial. In that case, the member may be in a post-buckling configuration, and this must be tested by *reducing* the starting slope still further by $\alpha/100$, to investigate the trend in the end deflection as described above.

The flow chart of Fig. 18 and Fig. 19 of the paper, and the accompanying discussion, illustrate these points.

* * *

NOTE: A detailed listing and documentation of the computer program are available at cost of reproduction from PCI Headquarters.

APPENDIX C — NUMERICAL EXAMPLES

In this section five numerical examples are given to show the application of the computer program.

EXAMPLE 1

Ref. 23 gives the results of several tests in which prestressed concrete piles were put under axial load and then loaded laterally to failure. The test shown in Fig. C1 was used as an example. The program is used to analytically check the stability of one of the piles tested and compare the results with the experimental values.

Input

All units are in kips and inches.

1972 Santa Fe Pomeroy 16 in. Pile Test (Title)

131111010	Program control
0.0	Controls on length intervals to be used in calculation, etc. — default values called for
4	No. of corners to concrete section
0.0	
16.0	x-coordinates of corners
16.0	
0.0	
0.0	
0.0	y-coordinates of corners
16.0	

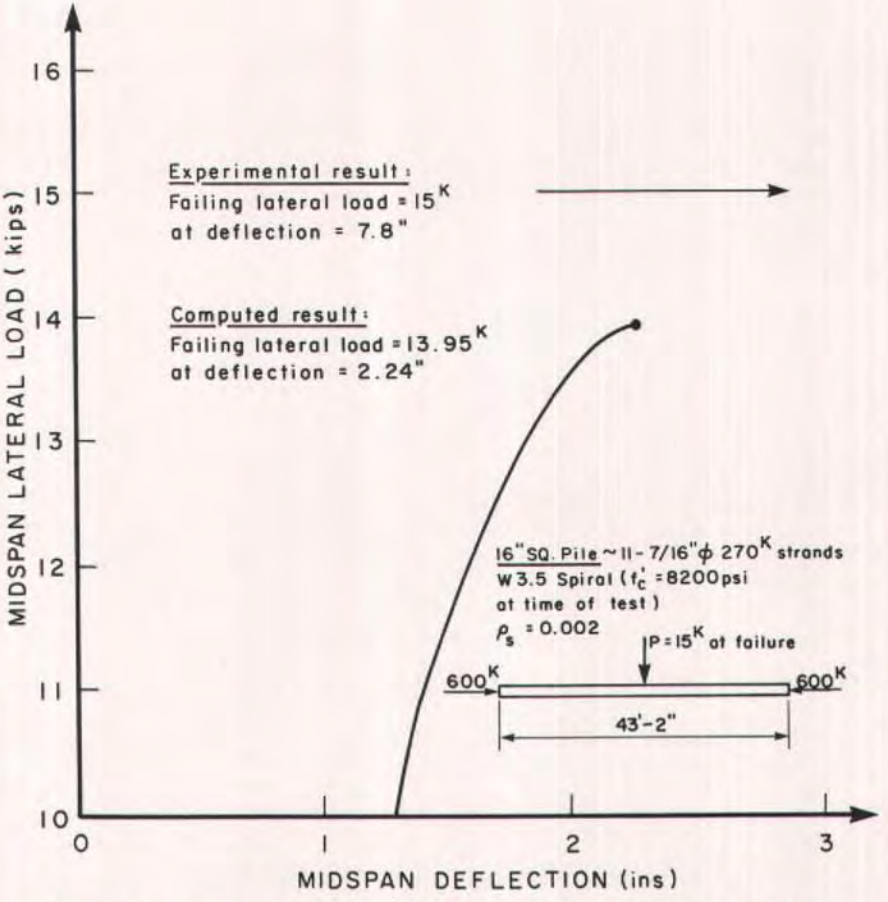

Fig. C1. Example 1. 1972 Santa Fe Pomeroy 16 in. pile test from Ref. 23.

16.0	
2	Concrete stress-strain law
8.2	Cylinder strength of concrete
0.002	Strain at peak stress
0.003	Strain at failure
0	No. of reinforcing bars
6	No. of prestressing tendons
0.115	
0.230	Areas of strands — One
0.230	strand plus five pairs
0.230	with equal y-coordinates
0.230	
0.230	
2.5	
3.373	
5.715	y-coordinates of strands
8.783	
11.602	
13.277	
2	Control indicating prestress is to be given as stress at zero concrete strain, i.e., after all losses except elastic shortening.
146.6	
146.6	
146.6	
146.6	Prestress
146.6	
146.6	
8	Stress-strain law for prestressing
270.0	Ultimate stress of prestressing strand
1	No. of axial loads
600.0	Axial load
1	No. of lengths
518.0	Length
0.0	
259.0	
518.0	Primary bending moment at tenth
777.0	points for lateral load of 10 kips.
1036.0	These will be increased in steps
1295.0	to failure.
1036.0	
777.0	
518.0	
259.0	
0.0	
0.0	Amplitude of initial crookedness
0.0	Eccentricity at starting end
0.0	Ratio of eccentricity at far end to that at starting end
1.0	Strength reduction factor in slenderness effects
1.0	Strength reduction factor on final results
0.0	Loading duration factor β_d

Output

The deflected shape of the member plus the bending moments are printed out.

Results

The results are shown on Fig. C1. Failure was reached at a lateral load of 13.95 kips due to instability. The deflection in the preceding step (13.90 kips) was 2.24 in. The experimental results gave failure at 15 kips and 7.8 in. However, this would indicate a midspan moment of:

$$M = (600)(7.8)/12 + (15)(43.17)/4$$
$$= 552 \text{ kip-ft}$$

This moment seems well beyond the capacity of the cross section, so it is probable that failure occurred at a lower deflection, the actual value of which would have been difficult to measure as the member became unstable.

Use of Formulas

To compute the actual strength of this member, without ϕ or β_d factors, the expressions of Ref. 15, p. 68 would have to be used. They are found to give $\lambda = 1.5$, $\delta = 7.59$, and maximum lateral load 4 kips. The unmodified ACI Code formula would give $P_{cr} = 415$ kips < 600 kips.

EXAMPLE 2

The load-moment relationships for six lengths and ten load values were computed for the double tee section of Fig. B3, with equal end eccentricities and no lateral load. The input was similar to that of Example 1, with different numbers in the program control card for the equal end eccentricity, failure load case.

The ACI Code strength reduction factor was used both in calculating slenderness effects and in reducing the short column capacity. The ratio β_d was set at

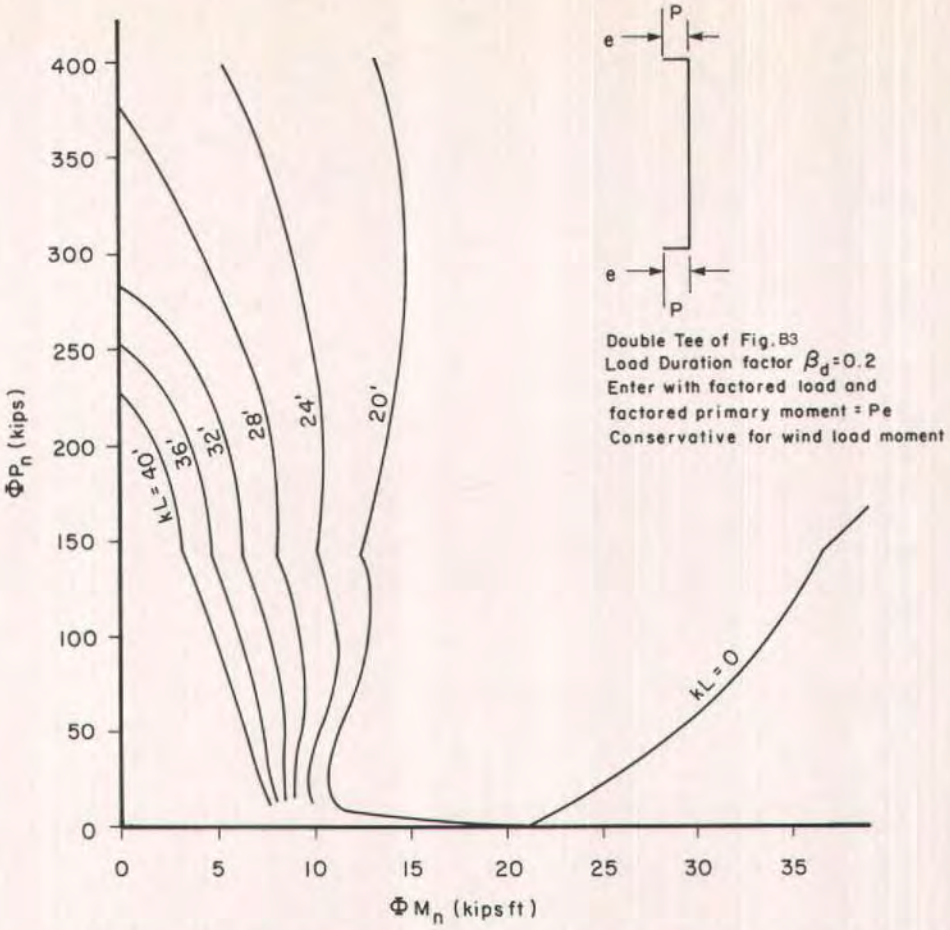

Fig. C2. Example 2. Design curve for double tee of Fig. B3. ACI strength reduction factors and load duration factor β_d = 0.2. Strands are assumed fully developed at points of high moment.

0.2. Fig. C2 shows the results in a form that might be provided by a precast manufacturer. The figure is a design chart for this member, similar to those given in Ref. 20, but including length effects.

The chart is entered with the factored loads and the factored primary moment: the interaction lines for the stated lengths define the safe values. If the primary moment arose from a parabolic wind load moment diagram instead of a constant Pe moment diagram, the results would be somewhat conservative.

EXAMPLE 3

Make the stability calculations for the column of Fig. C3; try the section shown in that figure.

Total factored load = 100 kips

Eccentricity at starting end (bottom) =

$$\frac{20 \text{ kip ft} \times 12}{100 \text{ kips}} = 2.4 \text{ in.}$$

Eccentricity at far end (top) = 0

Lateral load = 0

Strength reduction factor: ACI Code value

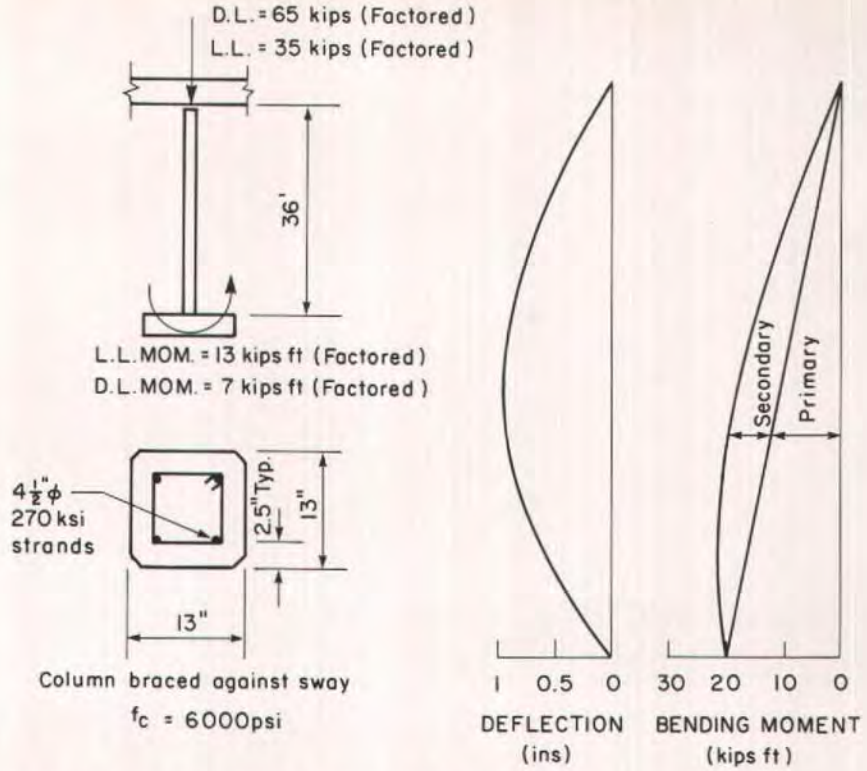

Fig. C3. Example 3. Braced prestressed concrete column.

Sustained load factor $\beta_d = 7/20 = 0.35$
Effective length factor = 1

The data are entered as for Example 1, and the column is found able to sustain the load with a maximum moment of 21.4 kip-ft.

The deflected shape and moment diagram are shown in Fig. C3. The column is apparently able to carry the factored loads with a substantial margin, but repeating the calculations with increasing load indicates that instability occurs as shown in Fig. C4.

Use of Formulas

A formula that covers the full range of section properties, slenderness values, and load durations must necessarily be conservative in most cases, if it is to be simple yet safe. A penalty must be paid for the use of simplified calculations. (Hence, the need for more accurate rational analyses as advocated herein.)

In this case, Eq. (11) indicates a larger, 15 in. square section. (With higher load duration factor β_d the approximate procedure becomes still more conservative.) Then:

$P_o = 1087$ kips
$P = 100$ kips
$P/P_o = 0.092$
$L/r = 96$
$\eta = 2.5 + 1.6/(P/P_o) = 19.9$
$\theta = 27/(L/r) - 0.05 = 0.231$
$\lambda = 4.60$
$EI = E_c I_c/\lambda(1 + \beta_d) = 3000000$ kip-in.^{2}
$P_c = 159$ kips
$\phi = 0.75$
$C_m = 0.6$

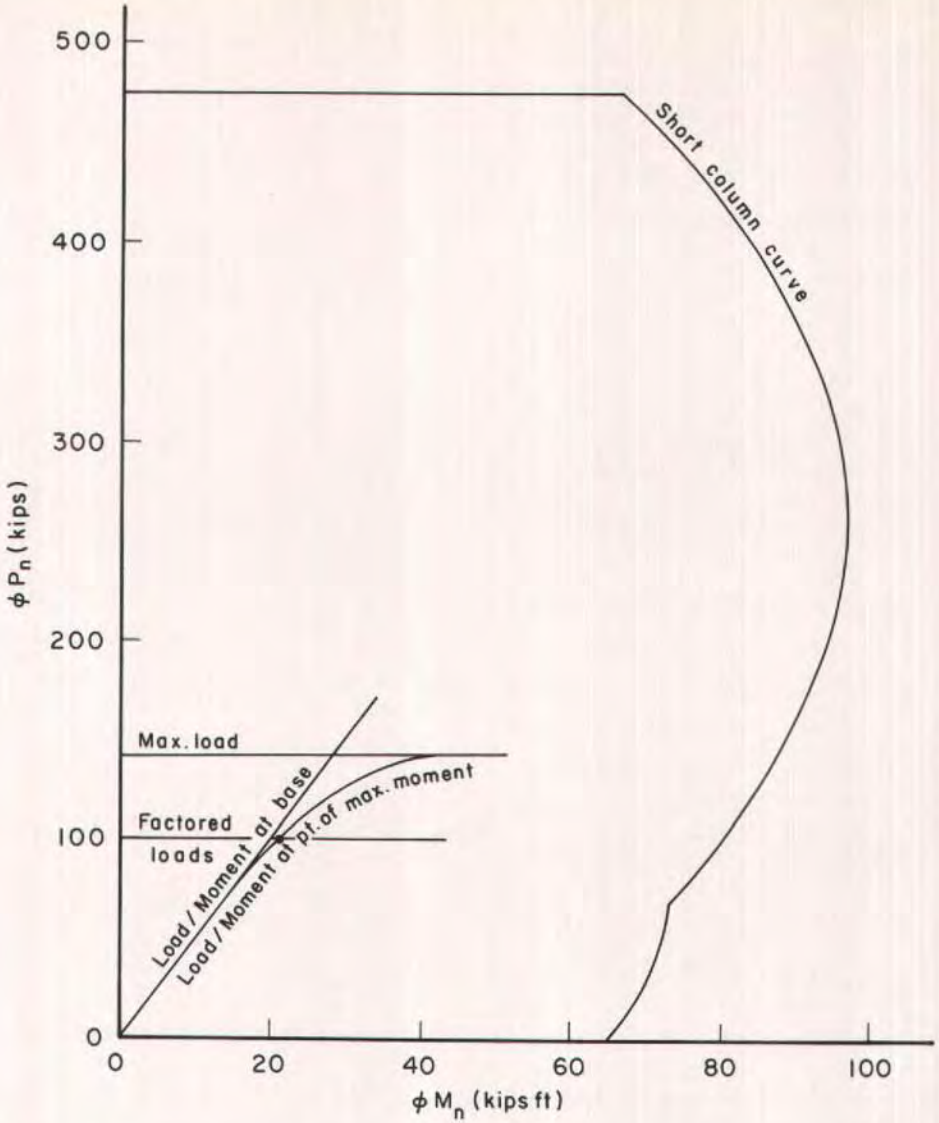

Fig. C4. Column of Example 3: proximity of instability failure belies appearance of excessive safety at magnified factored moment.

$\delta = C_m/1 - P/\phi P_c = 3.72$

$M = 20(3.72) = 74.4$ kip-in.

This moment is satisfactory for the 15 in. square section, but it is clear that this calculation greatly exaggerates the magnification of the moment. However, this discrepancy is intentional, reflecting the impending failure in instability as shown on Fig. C4.

The problem arises from the fact that a linear model is used to describe nonlinear behavior as discussed below Eq. (11), and as considered in detail in Ref. 15, in reference to Fig. 14 of that paper.

EXAMPLE 4

Make the stability calculations for the portal frame of Fig. C5, using the section of Fig. C3, with modified strand layout as indicated in Fig. C5.

Dead load on roof = 539 lbs/lin. ft

Live load on roof = 320 lbs/lin. ft

Loads on walls:

$P_D = 25(0.539) = 13.48$ kips/panel
$P_L = 25(0.320) = 8$ kips/panel

The two walls cantilever from the base, with the roof forming a pinned strut between them, carrying the compression necessary to equalize the deflections. Length changes in the roof unit could be included but will be assumed to be zero here, for clarity.

- **Primary Analysis at Service Loads:**

Let compression in roof member = F lbs

Deflection at roof level = $\frac{\omega L^4}{8EI} \pm \frac{FL^3}{3EI}$

(Use $E = 4000$ ksi, $I = 2872$ in.^{4})
Equate deflections at tops of walls:

$$\frac{160L^4}{8EI} - \frac{FL^3}{3EI} = \frac{128L^4}{8EI} + \frac{FL^3}{3EI}$$

$$F = 144 \text{ lbs}$$

$$\Delta_1 = \frac{160L^4}{8EI} - \frac{144L^3}{3EI}$$

$$= 0.90 \text{ in.}$$

- **Secondary Analysis at Service Loads:**

$$\text{Holding force } H = \frac{\Sigma P \Delta_1}{L}$$

$$\Delta_2 = \frac{HL^3}{3\Sigma EI}$$

$$= \frac{\Sigma P \Delta_1 L^2}{6EI}$$

$$= 0.05 \text{ in.}$$

No further iterations are necessary:
$\Delta = 0.95$ in.

- **Design Loads:**

Case 1. $U = 1.4D + 1.7L$
$P = 32.5$ kips
No wind loads

Case 2. $U = 0.75(1.4D + 1.7L + 1.7W)$
$P = 24.4$ kips
$W = 204$ plf (pressure)
163.2 plf (suction)

Case 3. $U = 0.9D + 1.3W$
$P = 12.13$ kips
$W = 208$ plf (pressure)
166.4 plf (suction)

Clearly, Case 2 governs.

Suppose that, under Case 2 loads, the moment of inertia of the section will be reduced by cracking to one-half of the initial value: say 1440 in.^{4} (This is the difficult part of this analysis; it should be done iteratively, with the assumed value being confirmed by calculation after the secondary moments are found.)

- **Primary Analysis at Design Loads:**

Equate deflections at tops of walls
(Use $E = 4000$ ksi, $I = 1440$ in.^{4})

$$\frac{204L^4}{8EI} - \frac{FL^3}{3EI} = \frac{163.2L^4}{8EI} + \frac{FL^3}{3EI}$$

$$F = 183.6 \text{ lbs}$$

$$\Delta_1 = \frac{204L^4}{8EI} - \frac{183.6L^3}{3EI}$$

$$= 2.28 \text{ in.}$$

- **Secondary Analysis at Design Loads:**

$$\text{Holding force } H = \frac{\Sigma P \Delta_1}{L}$$

$$\Delta_2 = \frac{HL^3}{3\Sigma EI}$$

$$= \frac{\Sigma P \Delta_1 L^2}{6EI}$$

$$= 0.27 \text{ in.}$$

$$\Delta_3 = \frac{\Sigma P \Delta_2 L^2}{6EI}$$

$$= 0.03 \text{ in.}$$

Accept: $\Delta = 2.58$ in.

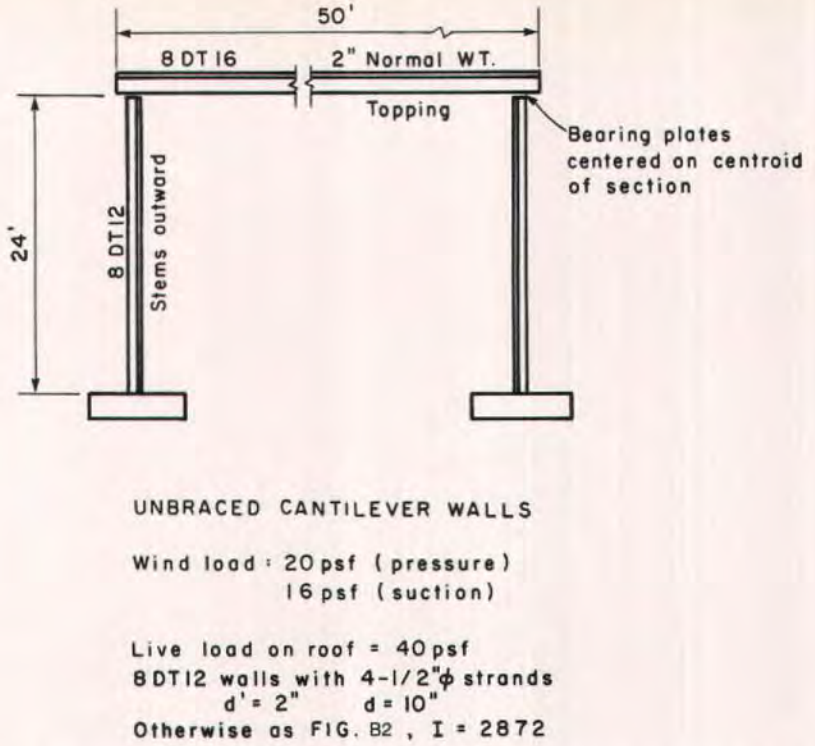

Fig. C5. Example 4. Portal frame with unbraced double tee cantilever wall units.

Moment at base of wall =
$(0.204)(24)^2/2 - (0.184)(24) + (24.4)(2.58)/12$
= 59.6 kip-ft

Moment capacity of section ϕM_n at ϕP_n = 24.4 kips, assuming strands are fully developed at the point of maximum moment, is calculated to be 63.3 kip-ft.

- **Moment Magnification**

It would ordinarily be necessary to account for additional moments due to departure of the column from the line joining the ends. This would be done by applying the moment magnification factor to the braced effective length, or by rational analysis, with the primary plus P-Δ moments. However, in the case of a cantilever column, the maximum moment is obviously at the base and this is not necessary.

Alternative Solution to Example 4 Using Program

The problem can be solved entirely by means of the computer program.

The load P is assumed to act vertically through the centroid of the concrete section at the top. At the bottom, it is set to some trial eccentricity. The data are then entered as for Example 1, with the primary moment due to the wind load and the calculated compression in the roof member.

The bottom is used as the starting end, and the slope there is examined. Examination of the curvature contours from the first run of the program shows that the member is cambered, with curvature at zero moment equal to 0.000032. It follows easily that the camber is 0.33 in. and the slope at the base of the unit would depart by 0.0046 from the verti-

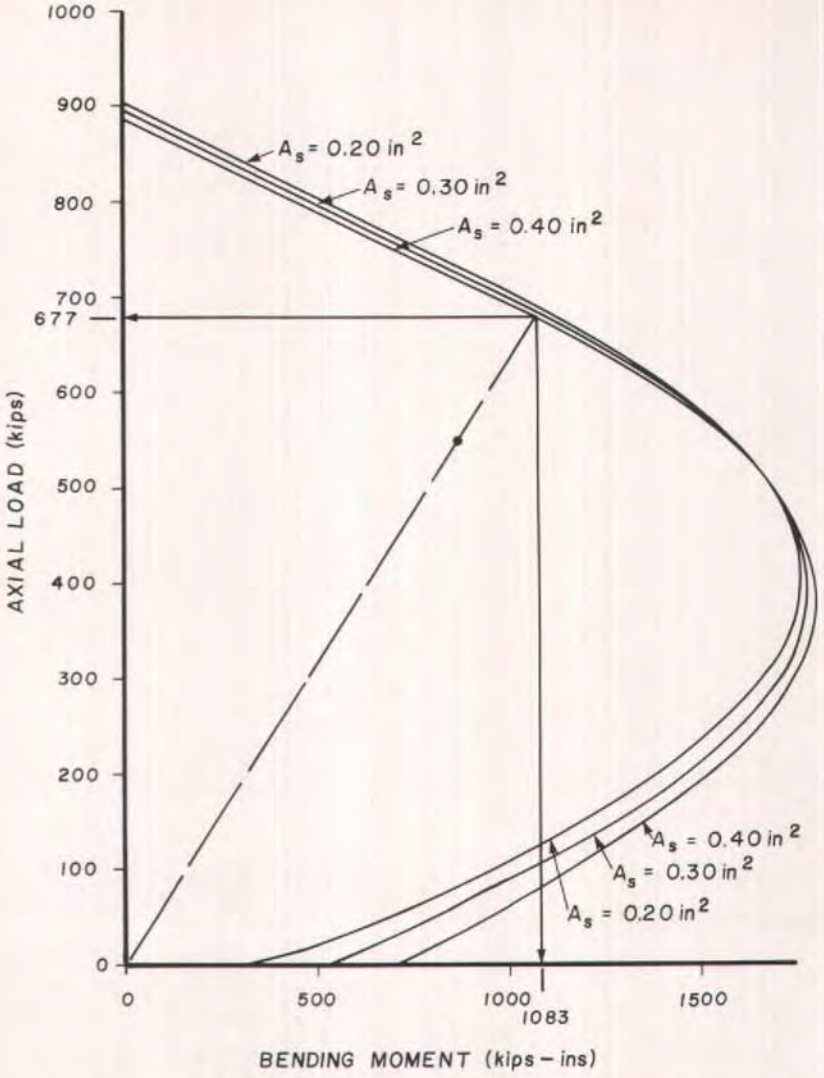

Fig. C6. Design data generated for Example 5. 16 in. square column with no length effects.

cal, if the unit were erected with the top of the section vertically above the bottom. The base eccentricity is varied in subsequent runs until this slope is achieved.

When the process is repeated for the leeward side, it is found that the tip deflections are not equal. This necessitates a change in the compression force assumed to act in the roof unit, to 50 lbs tension. The required balance is then obtained, with tip deflections equal to 2.20 in., and the maximum base moments equal to 64.4 kip-ft (windward) and 50.3 kip-ft (leeward).

It should be recalled that the manual P-Δ calculation above depended upon the value adopted for the moment of in-

ertia of the cracked section, which should have been calculated and corrected after the first trial. Thus, the apparent agreement is in part fortuitous, and in part due to the fact that the axial load is relatively small.

Note that this problem could usually be solved quite simply by using the effective length concept: by doubling the column length to include the mirror image below the foundation, with the axial load concentrically applied. The P-Δ effects would emerge naturally from such a calculation.

The difficulty in this case arose from the unsymmetric section with the consequent camber in the unloaded state. This means the mirror image column of effective length $2L$ would have had a slope discontinuity at midheight. Although manual calculations can ignore the camber, there does not appear to be any way of avoiding it in the more exact calculations.

Use of Formulas

Again, with use of the unbraced effective length of $2L$, moment magnification formulas should lead to the P-Δ moment. However, the L/r ratio for this member is 576/3.16 = 182, which is outside the range of applicability of any such formula. Thus, in this case, rational analysis of some form is mandatory.

EXAMPLE 5

A square prestressed concrete column is to be designed using the following data:

P_u = 550 kips	f_{pu} = 270 ksi
M_u = 875 kip-in.	f_{se} = 154.9 ksi
f'_c = 6 ksi	ϕ = 0.7

The minimum cover to the center of prestressing steel is 2 in.

This is Example 1 from Ref. 20, p. 138. As in that reference, a 16 in. square trial section was selected. The solution was obtained by running the program only as far as the ultimate strength interaction curve, since no length effects are involved.

Fig. C6 was obtained after a few minutes spent coding and running the program. As will be seen, it was concluded that the column was safe with four ⅜-in. diameter strands, giving a steel area of 0.34 in.^{2} At the given eccentricity, a load of 677 kips could be safely carried, with a moment of 1083 kip-in. These are exactly the results obtained in Ref. 20.

Note that the functional form used for the concrete stress-strain curve in Ref. 20 was not included in the program; nine points on the curve were calculated and entered, giving this result.

Slenderness effects could have been included by running the whole program. The design curves of Fig. C6 would then include length effects, as do those of Example 2 (Fig. C2).

* * *

Metric (SI) Conversion Factors

1 ft = 0.305 m	1 kip = 4.448 kN
1 in. = 25.4 mm	1 ksi = 6.895 MPa
1 in.^{2} = 645.2 mm^2	1 kip-in. = 113 N-m
1 in.^{4} = 416231 mm^4	1 kip-ft = 1356 N-m
1 lb = 4.448 N	1 psf = 0.0479 kPa